LETTER

doi:10.1038/nature17170

Hepatitis B virus X protein identifies the Smc5/6 complex as a host restriction factor

Adrien Decorsière[1]*, Henrik Mueller[1]†*, Pieter C. van Breugel[1]†*, Fabien Abdul[1]*, Laetitia Gerossier[2], Rudolf K. Beran[3], Christine M. Livingston[3], Congrong Niu[3], Simon P. Fletcher[3], Olivier Hantz[2] & Michel Strubin[1]

Chronic hepatitis B virus infection is a leading cause of cirrhosis and liver cancer[1,2]. Hepatitis B virus encodes the regulatory HBx protein whose primary role is to promote transcription of the viral genome, which persists as an extrachromosomal DNA circle in infected cells[3–5]. HBx accomplishes this task by an unusual mechanism, enhancing transcription only from extrachromosomal DNA templates[6]. Here we show that HBx achieves this by hijacking the cellular DDB1-containing E3 ubiquitin ligase to target the 'structural maintenance of chromosomes' (Smc) complex Smc5/6 for degradation. Blocking this event inhibits the stimulatory effect of HBx both on extrachromosomal reporter genes and on hepatitis B virus transcription. Conversely, silencing the Smc5/6 complex enhances extrachromosomal reporter gene transcription in the absence of HBx, restores replication of an HBx-deficient hepatitis B virus, and rescues wild-type hepatitis B virus in a DDB1-knockdown background. The Smc5/6 complex associates with extrachromosomal reporters and the hepatitis B virus genome, suggesting a direct mechanism of transcriptional inhibition. These results uncover a novel role for the Smc5/6 complex as a restriction factor selectively blocking extrachromosomal DNA transcription. By destroying this complex, HBx relieves the inhibition to allow productive hepatitis B virus gene expression.

HBx stimulates transcription of the hepatitis B virus (HBV) genome as well as of any reporter gene provided the DNA template remains extrachromosomal. When the template is integrated into the chromosome, the HBx effect is lost[4,6]. Previous studies suggested that this unusual property requires HBx to bind the DDB1 subunit of the DDB1-containing E3 ubiquitin ligase to target an unknown host cell factor for ubiquitin-mediated degradation[6–9]. To identify the HBx target(s), we employed a tandem affinity purification (TAP) strategy. As baits, we used wild-type HBx, a DDB1-binding-defective HBx(R96E) mutant[8], the woodchuck hepatitis virus HBx counterpart, WHx, that exhibits similar properties[8,10], and the unrelated paramyxovirus SV5-V protein. SV5-V binds DDB1 in a manner similar to HBx to target STAT1 for ubiquitin-mediated degradation[8,11,12]. DDB1 was the most abundant protein species co-purifying with all viral proteins, except the HBx(R96E) mutant (Extended Data Fig. 1a, b). Other components of the E3 ligase were also identified. This provides further evidence that HBx predominantly exists in association with the DDB1 E3 ligase complex[8,13,14]. However, no protein behaving as a potential HBx substrate was recovered. Similarly, STAT1 did not co-purify with SV5-V under these conditions (Extended Data Fig. 1b).

We therefore turned to an alternative strategy. We postulated that HBx may detectably interact with its substrate only when bound to DDB1 and when substrate ubiquitination is blocked. With this in mind, we took advantage of our previous finding that a covalent link between HBx and DDB1 forces interaction between the two proteins, thereby preventing HBx binding to endogenous DDB1[8,13]. We fused TAP-tagged HBx to wild-type DDB1 or to a DDB1 mutant that could not incorporate into the E3 ligase complex (Fig. 1a). The expectation was that fusion of HBx to the DDB1 mutant would prevent ubiquitination of the substrate and thereby stabilize the HBx–substrate interaction. A proof-of-principle experiment demonstrated that this did indeed occur with SV5-V and its target STAT1 (Extended Data Fig. 1c, d). Intriguingly, all six subunits of the Smc5/6 complex (Extended Data Fig. 1e), which plays a broad role in DNA repair and chromatin organization[15–17], were only recovered with the HBx–DDB1 mutant fusion (Fig. 1b and Supplementary Table 1). The selective recovery of this complex with the HBx–DDB1 mutant, and its lack of interaction with the corresponding SV5-V–DDB1 construct, was confirmed by co-immunoprecipitation experiments (Fig. 1c). Hence, the Smc5/6

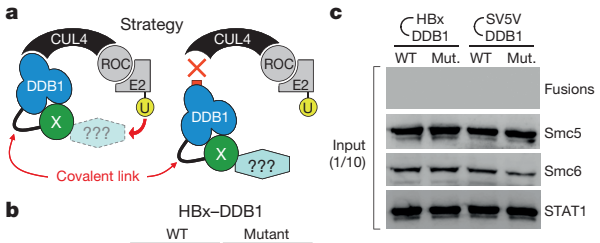

b HBx–DDB1

	WT		Mutant	
		Cov.		Cov.
HBx	Pep.	(%)	Pep.	(%)
HBx	2	18	3	28
DDB1 E3 ligase				
DDB1	39	38	34	35
DDA1	3	28	5	39
CUL4A	2	4	–	–
SMC complex				
Smc5	–	–	26	25
Smc6	–	–	17	22
Nse1	–	–	3	12
Nse2	–	–	7	23
Nse3	–	–	11	45
Nse4	–	–	2	6

Figure 1 | Identification of the Smc5/6 complex as an HBx interacting partner. a, Strategy. See text for description. **b**, The HBx–DDB1 fusions and associated proteins were isolated by TAP and subjected to mass spectrometric analysis (see Methods). The number of unique peptides (Pep.) and percentage of total protein sequence covered (Cov. (%)) are indicated. Nse1–4 are subunits of the Smc5/6 complex. WT, wild type. **c**, HBx and SV5-V fused to the indicated DDB1 were purified from transfected HepG2 cells. The amount recovered (IP) and the presence of Smc5, Smc6 and STAT1 (Co-IP) were assessed by western blot. The fusion proteins were detected using anti-Flag antibodies; expression was too low for detection in crude extracts (input). For gel source data, see Supplementary Fig. 1.

[1]Department of Microbiology and Molecular Medicine, University Medical Centre (C.M.U.), Rue Michel-Servet 1, 1211 Geneva 4, Switzerland. [2]CRCL, INSERM U1052, CNRS 5286, Université de Lyon, 151, Cours A Thomas, 69424 Lyon Cedex, France. [3]Gilead Sciences, Inc., 333 Lakeside Drive, Foster City, California 94404, USA. †Present addresses: Roche Pharmaceutical Research & Early Development, Infectious Diseases Discovery & Translational Area, Roche Innovation Center Basel, F. Hoffmann-La Roche Ltd, Grenzacherstrasse 124, 4070 Basel, Switzerland (H.M.); The Netherlands Cancer Institute, Division of Biological Stress Response, Plesmanlaan 121, 1066CX, Amsterdam, The Netherlands (P.C.v.B.).
*These authors contributed equally to this work.

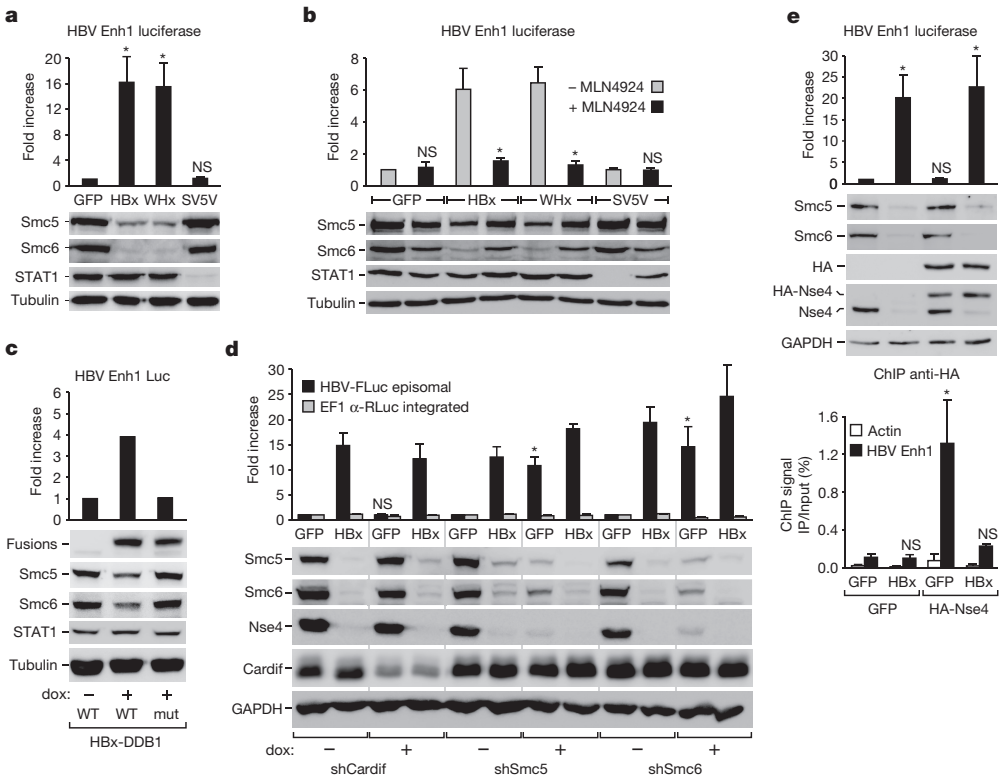

Figure 2 | HBx stimulates reporter gene activity by degrading Smc5/6 to prevent its binding to episomal DNA. a, HepG2 cells were transfected with a luciferase reporter gene driven by the HBV Enhancer I (Enh1) and then transduced with lentiviral vectors expressing green fluorescent protein (GFP) or the indicated GFP-tagged viral proteins. Luciferase assay and western blot were performed 6 days after transfection. Luciferase activity is relative to GFP, which was set to 1. $*P < 0.05$ by paired analysis of variance (ANOVA) relative to GFP control. NS, not significant ($P \geq 0.05$). **b**, Same as in **a** except cells were treated or not with 5 μM MLN4924 starting 6 h before transduction. Analysis was performed 3 days later. $*P < 0.05$ by *t*-test relative to matched no MLN4924 control. **c**, Same as in **a** but with cells expressing a doxycycline (dox)-inducible wild-type or mutant (mut) HBx–DDB1 fusion. Analysis performed as in **a**. See also Extended Data Fig. 2e. **d**, Activity of a transiently transfected (episomal) HBV Enh1-driven firefly reporter (HBV-FLuc) and a chromosomally integrated EF1α promoter-driven *Renilla* reporter (EF1α-RLuc) in HepG2 cells transduced with GFP or GFP–HBx and expressing (+) or not (−) the indicated doxycycline-inducible shRNA. Analysis performed after 6 days of culture. $*P < 0.05$ by *t*-test relative to matched HBV-FLuc episomal no doxycycline GFP control. **e**, Same as in **a** but with HepG2 cells co-transduced with GFP or an HA-tagged Nse4 subunit of the Smc5/6 complex together with GFP or GFP–HBx as indicated. Luciferase and western blot analyses performed 6 days later. In parallel, HA-Nse4 binding to the episomal reporter (filled bars) or the β-actin gene (open bars) was monitored by ChIP using anti-HA antibodies (bottom). Data expressed as percentage of input DNA recovered. Note the reduced binding of HA-Nse4 in the presence of HBx despite comparable expression levels, consistent with the protein associating to DNA only when incorporated into the Smc5/6 complex. See also Extended Data Fig. 3c. $*P < 0.05$ by paired ANOVA relative to GFP control. Data in **a**, **b**, **d** and **e** are mean ± s.e.m.; $n = 3$ independent experiments.

complex behaves as STAT1 in the SV5-V experiment, strongly suggesting that the complex is a substrate of HBx.

This hypothesis and the key role of the Smc5/6 complex in mediating the HBx stimulatory activity were confirmed as follows. Western blot analysis revealed that Smc5 and Smc6 levels were strongly decreased in HepG2 cells expressing HBx (Fig. 2a). The same was observed with the woodchuck WHx, suggesting a conserved mechanism (Fig. 2a). This correlated with the stimulatory effects of HBx and WHx on the activity of a transiently transfected luciferase reporter construct, which, like the HBV genome, remains extrachromosomal[6]. In contrast, SV5-V triggered degradation of STAT1 but had no effect on Smc5 or Smc6 levels or reporter gene expression (Fig. 2a). HBx-mediated depletion of Smc6 was rapid, occurring concomitantly with or preceding the HBx-mediated increase in reporter gene expression (Extended Data Fig. 2a), and was inhibited by exposure to the proteasome inhibitor MG132 (Extended Data Fig. 2b), consistent with a role of proteasomes in HBx activity[18]. HBx and WHx had no impact on Smc5 and Smc6 messenger RNA levels, excluding an effect on transcription or mRNA stability (Extended Data Fig. 2c). Furthermore, pre-treatment of cells with MLN4924, an inhibitor of the E3 ubiquitin ligase family to which the DDB1 E3 ligase belongs[19,20], abrogated the effects of HBx and WHx both on reporter gene activity and on Smc5 and Smc6 protein levels (Fig. 2b and Extended Data Fig. 2d). This implicates the DDB1 E3 ubiquitin ligase activity in HBx function. Consistently, HBx retained transactivation activity and the ability to decrease Smc5 and Smc6 protein levels when fused to wild-type DDB1 but not to the mutant that cannot incorporate into the E3 ligase (Fig. 2c and Extended Data Fig. 2e).

The above results are consistent with HBx and WHx using the DDB1 E3 ubiquitin ligase to target the Smc5/6 complex for ubiquitin-mediated proteasome degradation. They further suggest that this event explains the stimulatory effect of HBx on extrachromosomal reporter gene activity. To test the latter hypothesis, we monitored the consequence of depleting Smc5 or Smc6 by RNA interference. HepG2 cell lines were generated to express doxycycline-inducible short hairpin (sh) RNA targeting Smc5, Smc6, or Cardif (MAVS) as a control. Dual *Renilla* and firefly luciferase reporter genes driven by unrelated promoters were tested in pairwise combinations in these cells, with one being integrated into the chromosomes and the other transiently transfected, and therefore episomal. All three reporter constructs tested responded to HBx only as episomal templates (Fig. 2d and Extended Data Fig. 2f, g). This was consistent with our earlier observation that HBx stimulates extrachromosomal DNA templates selectively and independently of promoter type[6]. Depletion of Smc5 or Smc6, which destabilizes the

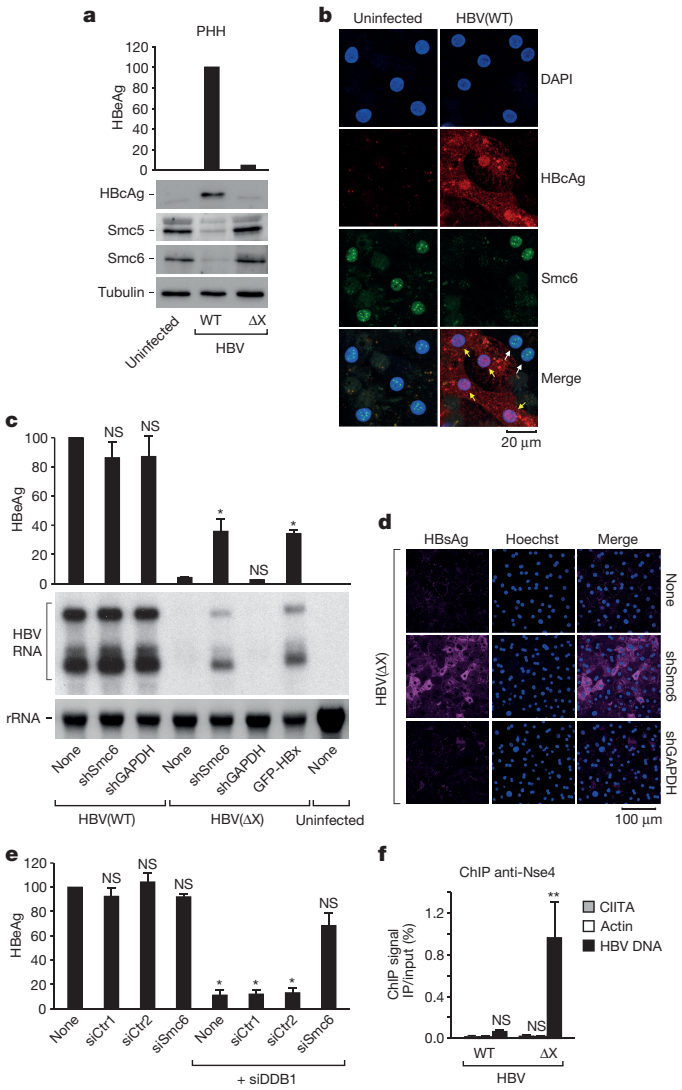

Figure 3 | HBx promotes HBV transcription in PHHs by preventing Smc5/6 binding to the viral genome. a, Purified PHHs were left uninfected or infected with wild-type or HBx-deficient (ΔX) HBV. HBeAg secretion, a marker for HBV gene expression, and indicated proteins were quantified 10 days later by ELISA and western blot. HBcAg is the viral capsid. HBeAg concentrations are relative to wild-type HBV, which was set to 100. See also Extended Data Fig. 6a. **b**, Confocal microscopy of control (left) and HBV-infected (right) PHHs stained for HBcAg (red) and Smc6 (green). Cell nuclei visualized with 4′,6-diamidino-2-phenylindole (DAPI, blue). HBcAg-positive and -negative cells are indicated by yellow and white arrows, respectively. See also Extended Data Fig. 7. **c**, PHHs were mock transduced (none) or transduced 1 day before HBV infection with indicated shRNAs or GFP–HBx. HBeAg secretion and viral RNA production were assessed 8 days later by ELISA and northern blot. Mean ± s.e.m.; $n = 4$ independent experiments with three different PHH donors. $^{*}P < 0.05$ by paired ANOVA relative to matched no shRNA control (none). **d**, Same as in **c** but cells infected with HBx-mutant HBV were examined for surface antigen (HBsAg) positivity 12 days after infection. Cell nuclei stained with Hoechst dye (blue). **e**, PHHs were mock transfected (none) or transfected with indicated siRNAs 4 days before HBV infection. HBeAg secretion was measured 13 days later. Mean ± s.e.m.; $n = 4$ independent experiments with two different PHH donors. $^{*}P < 0.05$ by paired ANOVA relative to no siRNA control (none). **f**, PHHs were infected as indicated. At 10 days after infection, the binding of Smc5/6 to repressed CIITA and active β-actin genes, and to episomal HBV DNA was monitored by ChIP using anti-Nse4 antibodies. Mean ± s.e.m.; $n = 3$ independent experiments with different PHH donors and virus stocks. $^{**}P < 0.01$ by unpaired ANOVA relative to WT HBV β-actin control.

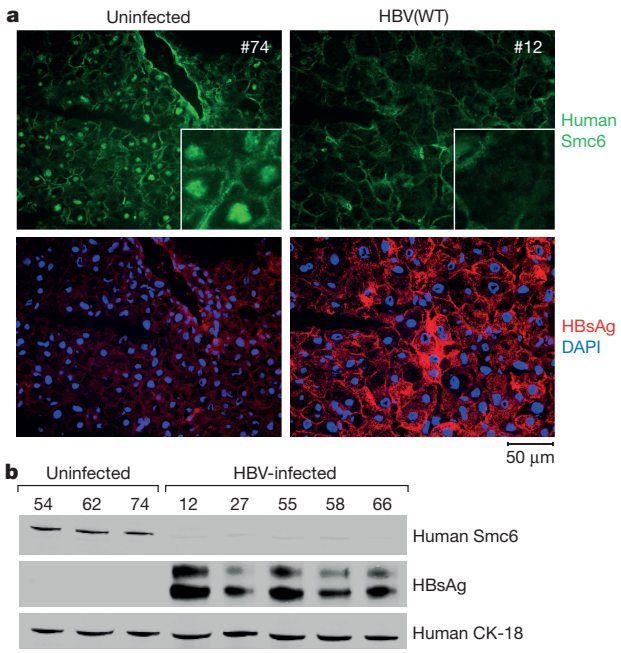

Figure 4 | HBV infection induces Smc6 degradation in humanized mouse liver tissue. a, Fresh-frozen liver tissue sections from the indicated humanized mice were stained for human Smc6 (green) and HBsAg (red). Blue, DAPI. Insets represent a digital zoom of selected areas. Note the absence of Smc6 nuclear staining in the HBV-infected tissue. See also Extended Data Figs 8 and 9. Images are representative of six HBV-infected and three uninfected humanized mice. **b**, Western blot analysis for human Smc6 and HBsAg expression in the indicated humanized liver samples. Human cytokeratin-18 (CK-18) served as a control.

entire Smc5/6 complex[21], stimulated expression of the three episomal constructs to levels approaching those measured in the presence of HBx, but remained without effect on the corresponding chromosomal reporters (Fig. 2d and Extended Data Fig. 2f, g). This recapitulated exactly the situation observed with HBx. Moreover, knockdown of Smc5 or Smc6 had no further effect on transcription stimulated by HBx, consistent with activation by HBx and by Smc5/6 knockdown occurring through the same pathway. HBx-mediated destruction of the Smc5/6 complex, which has been involved in cell cycle progression and recombinational DNA repair[22–24], did not alter the cell cycle or induce integration of the reporter gene into the chromosomes (Extended Data Fig. 3a, b). Instead, chromatin immunoprecipitation (ChIP) analysis revealed that the Smc5/6 complex binds to transiently transfected reporter plasmids but not to a chromosomally integrated reporter, and that HBx reduces this binding (Fig. 2e and Extended Data Fig. 3c). This is in line with recent *in vitro* studies[25]. Thus, HBx stimulates gene transcription mainly, if not exclusively, by triggering degradation of the Smc5/6 complex to prevent its association with episomal DNA templates.

The importance of these findings for HBV replication was examined using an infection assay of primary human hepatocytes (PHHs). In this assay, mutant HBV lacking a functional HBx gene is fully competent to enter cells and deliver its circular DNA genome into the nucleus. However, no viral gene transcription is detected[4] (Fig. 3c and Extended Data Fig. 4a). We observed that cells infected at high efficiency (Extended Data Fig. 5) with wild-type HBV displayed decreased levels of Smc5 and Smc6, but not when infected with an HBx-defective virus (Fig. 3a, b and Extended Data Figs 6a and 7). Conversely, depletion of Smc6 by shRNA (Extended Data Fig. 6b) restored replication competency to the HBx-deficient virus without affecting genome copy number (Extended Data Fig. 4b) but had no effect on replication of the wild-type virus (Fig. 3c, d and Extended Data Fig. 6c). The same was observed in HBV-permissive HepaRG

cells (Extended Data Fig. 6d). Furthermore, siRNA-mediated silencing of DDB1 blocked HBV transcription, and this effect was relieved by the concomitant downregulation of Smc6 or Smc5 (Fig. 3e and Extended Data Fig. 6e–i). Thus, a major function of the HBx–DDB1 E3 ligase interaction is to target the Smc5/6 complex for destruction. ChIP analysis demonstrated that the Smc5/6 complex also associates with the HBV episomal DNA genome, and that binding was reduced in the presence of HBx (Fig. 3f).

In summary, our results indicate that the Smc5/6 complex binds episomal DNA templates and inhibits their transcription. HBx, by destroying the complex, relieves the inhibition to allow productive HBV gene expression. Further supporting this notion, HBV-infected humanized mouse liver tissues show markedly reduced levels of Smc6 (Fig. 4 and Extended Data Figs 8 and 9). This points to a novel role for the Smc5/6 complex as a host restriction factor, and offers a potential new avenue for therapeutic intervention against HBV infection. The Smc5/6 complex is, together with condensin and cohesin, one of the three related Smc complexes identified in eukaryotes[26]. These complexes share a similar architecture and play fundamental roles in chromosome organization, segregation, and repair (reviewed in ref. 27). The Smc5/6 complex has well-recognized functions in homologous recombination-mediated DNA repair[15,16]. In addition, the complex has been implicated in DNA replication, chromosome topology, and transcription, but little is known of its precise function[15–17,24]. A role in host defence against viral infection has not previously been reported. It will be interesting to determine whether the restrictive activity of the Smc5/6 complex is connected to any of its cellular functions, and whether the complex exhibits antiviral activity against other episomal DNA viruses.

Online Content Methods, along with any additional Extended Data display items and Source Data, are available in the online version of the paper; references unique to these sections appear only in the online paper.

Received 5 February 2014; accepted 27 January 2016.

1. Seeger, C. & Mason, W. S. Hepatitis B virus biology. *Microbiol. Mol. Biol. Rev.* **64,** 51–68 (2000).
2. Ganem, D. & Prince, A. M. Hepatitis B virus infection — natural history and clinical consequences. *N. Engl. J. Med.* **350,** 1118–1129 (2004).
3. Benhenda, S., Cougot, D., Buendia, M. A. & Neuveut, C. Hepatitis B virus X protein molecular functions and its role in virus life cycle and pathogenesis. *Adv. Cancer Res.* **103,** 75–109 (2009).
4. Lucifora, J. *et al.* Hepatitis B virus X protein is essential to initiate and maintain virus replication after infection. *J. Hepatol.* **55,** 996–1003 (2011).
5. Feitelson, M. A., Bonamassa, B. & Arzumanyan, A. The roles of hepatitis B virus-encoded X protein in virus replication and the pathogenesis of chronic liver disease. *Expert Opin. Ther. Targets* **18,** 293–306 (2014).
6. van Breugel, P. C. *et al.* Hepatitis B virus X protein stimulates gene expression selectively from extrachromosomal DNA templates. *Hepatology* **56,** 2116–2124 (2012).
7. Leupin, O., Bontron, S., Schaeffer, C. & Strubin, M. Hepatitis B virus X protein stimulates viral genome replication via a DDB1-dependent pathway distinct from that leading to cell death. *J. Virol.* **79,** 4238–4245 (2005).
8. Li, T., Robert, E. I., van Breugel, P. C., Strubin, M. & Zheng, N. A promiscuous α-helical motif anchors viral hijackers and substrate receptors to the CUL4-DDB1 ubiquitin ligase machinery. *Nature Struct. Mol. Biol.* **17,** 105–111 (2010).
9. Hodgson, A. J., Hyser, J. M., Keasler, V. V., Cang, Y. & Slagle, B. L. Hepatitis B virus regulatory HBx protein binding to DDB1 is required but is not sufficient for maximal HBV replication. *Virology* **426,** 73–82 (2012).
10. Sitterlin, D., Bergametti, F. & Transy, C. UVDDB p127-binding modulates activities and intracellular distribution of hepatitis B virus X protein. *Oncogene* **19,** 4417–4426 (2000).
11. Ulane, C. M. & Horvath, C. M. Paramyxoviruses SV5 and HPIV2 assemble STAT protein ubiquitin ligase complexes from cellular components. *Virology* **304,** 160–166 (2002).
12. Precious, B., Childs, K., Fitzpatrick-Swallow, V., Goodbourn, S. & Randall, R. E. Simian virus 5 V protein acts as an adaptor, linking DDB1 to STAT2, to facilitate the ubiquitination of STAT1. *J. Virol.* **79,** 13434–13441 (2005).
13. Leupin, O., Bontron, S. & Strubin, M. Hepatitis B virus X protein and simian virus 5 V protein exhibit similar UV-DDB1 binding properties to mediate distinct activities. *J. Virol.* **77,** 6274–6283 (2003).
14. Benhenda, S. *et al.* Methyltransferase PRMT1 is a binding partner of HBx and a negative regulator of hepatitis B virus transcription. *J. Virol.* **87,** 4360–4371 (2013).
15. Murray, J. M. & Carr, A. M. Smc5/6: a link between DNA repair and unidirectional replication? *Nature Rev. Mol. Cell Biol.* **9,** 177–182 (2008).
16. De Piccoli, G., Torres-Rosell, J. & Aragón, L. The unnamed complex: what do we know about Smc5-Smc6? *Chromosome Res.* **17,** 251–263 (2009).
17. Jeppsson, K., Kanno, T., Shirahige, K. & Sjögren, C. The maintenance of chromosome structure: positioning and functioning of SMC complexes. *Nature Rev. Mol. Cell Biol.* **15,** 601–614 (2014).
18. Zhang, Z., Sun, E., Ou, J. H. & Liang, T. J. Inhibition of cellular proteasome activities mediates HBX-independent hepatitis B virus replication *in vivo*. *J. Virol.* **84,** 9326–9331 (2010).
19. Soucy, T. A. *et al.* An inhibitor of NEDD8-activating enzyme as a new approach to treat cancer. *Nature* **458,** 732–736 (2009).
20. Emanuele, M. J. *et al.* Global identification of modular cullin-RING ligase substrates. *Cell* **147,** 459–474 (2011).
21. Taylor, E. M., Copsey, A. C., Hudson, J. J., Vidot, S. & Lehmann, A. R. Identification of the proteins, including MAGEG1, that make up the human SMC5-6 protein complex. *Mol. Cell. Biol.* **28,** 1197–1206 (2008).
22. Kegel, A. & Sjögren, C. The Smc5/6 complex: more than repair? *Cold Spring Harb. Symp. Quant. Biol.* **75,** 179–187 (2010).
23. Potts, P. R., Porteus, M. H. & Yu, H. Human SMC5/6 complex promotes sister chromatid homologous recombination by recruiting the SMC1/3 cohesin complex to double-strand breaks. *EMBO J.* **25,** 3377–3388 (2006).
24. Tapia-Alveal, C., Lin, S. J. & O'Connell, M. J. Functional interplay between cohesin and Smc5/6 complexes. *Chromosoma* **123,** 437–445 (2014).
25. Kanno, T., Berta, D. G. & Sjögren, C. The Smc5/6 complex is an ATP-dependent intermolecular DNA linker. *Cell Reports* **12,** 1471–1482 (2015).
26. Aragon, L., Martinez-Perez, E. & Merkenschlager, M. Condensin, cohesin and the control of chromatin states. *Curr. Opin. Genet. Dev.* **23,** 204–211 (2013).
27. Hirano, T. At the heart of the chromosome: SMC proteins in action. *Nature Rev. Mol. Cell Biol.* **7,** 311–322 (2006).

Supplementary Information is available in the online version of the paper.

Acknowledgements We are most grateful to M. Rivoire for providing liver samples, L. Lefrancois and M. Michelet for help in preparing hepatocytes, U. Protzer for the HBV(ΔX)-producing cell line, C. J. Gloeckner for the StrepII/Flag TAP-tag construct, C. E. P. Goldring for the tetracyclin-inducible HepG2 cell line, S. Elledge for the lentiviral pINDUCER vectors, A. R. Lehmann for anti-Smc5 and anti-Smc6 antibodies, M. A. Petit for anti-HBsAg and anti-HBcAg antibodies, D. Garcin for the Cardif shRNA construct, Q. Seguín-Estévez, Y. Grimaldi and P. Ferrari for help with the ChIP assay, P. Arboit and the Geneva Proteomics Core Facility for mass spectrometry analysis, the Centre d'imagerie Quantitative Lyon-Est for help in confocal microscopy, A. Joshi for statistical analysis support, and J. Curran for reading the manuscript. This study was supported by grants from CLARA (Lyon) and the French National Agency for Research against AIDS and viral hepatitis (ANRS) (to O.H.) and from the Swiss National Science Foundation (31003A-127384 and 310030-149626) (to M.S.) and by the Canton of Geneva (to M.S).

Author Contributions A.D. performed the experiments shown in Figs 1c and 2c–e and Extended Data Figs 2e–g and 3b, c, and performed the ChIP assay in Fig. 3f. H.M. performed the experiments shown in Fig. 2a, b and Extended Data Fig. 2a, d. P.C.v.B. established the TAP approach and performed the experiments shown in Fig. 1b and Extended Data Fig. 1. F.A. performed the experiments in Extended Data Figs 2b, c and 3a, c, the western blots in Fig. 3a and Extended Data Fig. 6b, and contributed to Fig. 2e and Extended Data Fig. 3c. O.H. and L.G. performed the PHH infection experiments in Fig. 3a, c, d and Extended Data Figs 4, 5 and 6a–c, the HepaRG experiment in Extended Data Fig. 6d, and contributed to Fig. 3f. C.M.L. performed the confocal and epifluorescence microscopy experiments in Figs 3b and 4a and Extended Data Figs 7–9 and contributed to Fig. 4b. C.N. and R.K.B. performed the PHH experiments in Fig. 3e and Extended Data Fig. 6e, f, h, i. R.K.B. performed the western blots in Fig. 4b and Extended Data Fig. 6g and contributed to Fig. 3f. All authors designed the experiments and interpreted the results. M.S. wrote the paper with input from all authors.

Author Information Reprints and permissions information is available at www.nature.com/reprints. The authors declare competing financial interests: details are available in the online version of the paper. Readers are welcome to comment on the online version of the paper. Correspondence and requests for materials should be addressed to O.H. (olivier.hantz@inserm.fr), S.P.F. (Simon.Fletcher@gilead.com) or M.S. (michel.strubin@unige.ch).

METHODS

Expression plasmids. HBx fused at its carboxy (C) terminus via a 10-amino-acid linker (HMRSRSGLET) either to wild-type DDB1 or to the CUL4-binding-defective DDB1 mutant has been described[8,28]. The SV5-V–DDB1 fusions were generated by replacing the sequence encoding HBx within the HBx–DDB1 fusions by the full-length SV5-V coding region[13]. Unless fused to DDB1, all viral proteins contain an amino (N)-terminal GFP tag and have been described[6]. For TAP, the proteins carried an N-terminal Flag tag followed by two Strep-tag II sequences (FS-tag)[29]. For ChIP analysis, the full-length NSE4a coding region was amplified by PCR from a Namalwa B cell complementary DNA (cDNA) library and fused N-terminal to three tandem copies of the HA epitope. Proteins were expressed from a stably integrated tetracycline-inducible pTRE2hyg plasmid vector (Clontech) in Fig. 1b and Extended Data Fig. 1a, b, from the episomal Epstein–Barr virus-based expression vector EBS-PL[30] in Fig. 1c and Extended Data Fig. 1d, from the tetracycline-inducible lentiviral vector pINDUCER20 (ref. 31) (a gift from S. Elledge) in Fig. 2c and Extended Data Fig. 2e, and from the lentivirus vector pWPT[6,7] in all the other figures.

Luciferase reporter constructs. The luciferase reporter genes were constructed into pcDNA3 (pGL3 in the case of HBV Enhancer I[6]) for transient transfection and into the self-inactivating lentiviral vector pWPT (pWPXL in the case of HBV Enhancer I[6]) for chromosomal integration. In Extended Data Fig. 3c, the EF1α episomal reporter was delivered using an integrase-defective (D116A) lentiviral vector[32].

RNA interference. The short hairpin RNAs (shRNAs) used for Smc5 and Smc6 knockdown were cloned into the miR30 context as 116-nucleotide XhoI–EcoRI fragments into pINDUCER10 (ref. 31) and/or pGIPZ (Open Biosystems) lentiviral vectors. The sequences were as follows, with the hairpin sequence in capital letters and flanking miR30 sequences shaded in bold type: shSmc5(1), **gagcg**GTGAGGTGAAAGAAGTGTTTCTtagtgaagccacagatgtaAGAAACACTTC TTTCACCTCAT**tgcct**; shSmc5(2), **gagcg**GTGCGAAACTTGTTACCGAATT tagtgaagccacagatgtaAATTCGGTAACAAGTTTCGCAT**tgcct**; shSmc6(1), **gagcg**GTGAGCAGCTTTGTAAACGAATtagtgaagccacagatgtaATTCGTTTACAA AGCTGCTCAT**tgcct**; shSmc6(2) (from Thermo Scientific (V3LHS_325916), **gagcg**CAGAGACAGTGCTACTAATCAAtagtgaagccacagatgtaTTGATTAGTAG CACTGTCTCTA**tgcct**.

The constructs used were shSmc5(2) and shSmc6(1) in Fig. 2d, shSmc5(1) and shSmc6(2) in Extended Data Fig. 2f, and shSmc6(2) in Extended Data Fig. 2g. The Cardif shRNA construct in pINDUCER10 was a gift from D. Garcin. The GAPDH shRNA construct in pGIPZ was purchased from Thermo Scientific (RHS4371). Expression was from pINDUCER10 in Fig. 2d and Extended Data Fig. 2f, g and from pGIPZ in Fig. 3c, d. Details of plasmid constructions are available upon request. The sequences of the siRNAs used in the other figures can be found in Supplementary Table 2.

Cell culture and establishment of stable cell lines. The human hepatoma cell lines HepG2 (ATCC HB-8065), HepG2$^{tet\text{-}on}$ (ref. 33), and derivatives were grown at 37 °C under 5% CO_2 in modified Eagle's medium (MEM; Life Technologies or Sigma-Aldrich) supplemented with 10% (vol/vol) fetal calf serum (Gibco), 1% (v/v) penicillin/streptomycin solution, 2 mM L-glutamine, 1 mM sodium pyruvate, and 0.1 mM MEM non-essential amino acids solution (all from Life Technologies). In Extended Data Fig. 6d, HepaRG cells were cultured, induced to differentiate, and infected with HBV as described[34]. The cell lines were not authenticated or tested for *Mycoplasma* contamination because of their direct purchase from ATCC or low passage number.

The stable HepG2 cell lines used in Fig. 1b and Extended Data Fig. 1a, b that expressed the tetracycline-inducible transactivator rtTA and various FS-tagged proteins from a tetracycline-responsive promoter were established as follows. The HepG2$^{tet\text{-}on}$ parental cell line[33] was plated at a density of 1×10^5 cells per 6-cm dish and transfected using FuGENE HD (Roche) with the relevant constructs cloned into pTRE2hyg (Clontech), which carries a hygromycin resistance marker. At day 3 after transfection, cells were selected in medium containing 250 μg ml^{-1} hygromycin B (PAA Laboratories) and 100 μg ml^{-1} G418 (Geneticin, Gibco)[33]. Resistant colonies were picked and expanded in 48-well plates under the same selection conditions. Individual clones were assayed by reverse transcription (RT)-PCR and western blot analyses for transgene expression in the presence or absence of 2 μg ml^{-1} doxycycline (Sigma Aldrich).

The HepG2 cells in Fig. 2c expressing the doxycycline-inducible HBx–DDB1 fusions from pINDUCER20 lentiviral vector carrying a neomycin resistance marker were obtained by selection for 2 days with 1 mg ml^{-1} G418 (Promega) starting at day 3 after transduction.

The HepG2 cells in Fig. 2d and Extended Data Fig. 2f, g expressing doxycycline-inducible shRNAs against Smc5, Smc6, or Cardif from pINDUCER10 lentiviral vector were obtained by selection with 10 μg ml^{-1} puromycin (Calbiochem) for 4 days starting at day 3 after transduction. The resulting puromycin-resistant cells were then cultured for 2 weeks in the absence or presence of 2.5 μg ml^{-1} doxycycline before transduction of GFP or GFP–HBx to maximally induce shRNA expression. Fluorescence microscopy indicated that >90% of the cells were expressing turboRFP (tRFP) from the tRFP-shRNA cassette[31].

The HepG2.2.15 (ref. 4), HepAD38 (ref. 35), and HepG2-H1.3x- (ref. 4) stable cell lines used to produce HBV virions carrying either a wild-type genome or a genome bearing a defective HBx gene have been described. They were maintained in Dulbecco's modified Eagle's medium/F-12 (DMEM/F12) complemented with 10% fetal calf serum, 1% non-essential amino acids, 50 μg ml^{-1} kanamycin, and 200 μg ml^{-1} geneticin.

Transfection, transduction, and reporter gene assay. Transfection of plasmid DNA in HepG2 cells was performed using X-tremeGENE HP DNA Transfection Reagent (Roche) following the manufacturer's instructions. Transfection of siRNA duplexes in HepaRG cells was performed using DharmaFECT-1 (Thermo Scientific) transfection reagent and in PHHs using Lipofectamine RNAiMax (Life Technologies). Recombinant lentivirus production and transduction of HepG2 cells were performed as described previously[7,36]. For PHH transduction, lentivirus supernatants were concentrated by ultracentrifugation at 130,000 *g* for 1 h in a SW32 Beckman rotor at 4 °C and transduction was performed overnight in the presence of 10 ng ml^{-1} of EGF[37]. For luciferase reporter gene assay and western blot analysis, cells were typically seeded at a density of about 6×10^5 cells per 30 mm diameter well (1×10^5 cells per square centimetre) and transfected the next day with 30 ng of reporter plasmid DNA and 2 μg of empty EBS-PL vector. For the ChIP experiment in Fig. 2e, 3 or 30 ng of reporter plasmid were used with similar results.

In Fig. 2d and Extended Data Fig. 2f, g, cells that had been cultured in the absence or presence of doxycyclin for 2 weeks to induce shRNA expression from pINDUCER10 were first transduced and the next day transfected with, respectively, lentiviral and plasmid constructs carrying the *Renilla* and firefly luciferase reporter genes as indicated in the figures. Cells were trypsinized the following day, washed with phosphate-buffered saline (PBS), replated in 6- or 24-well dishes at a density of about 6×10^4 cells per square centimetre and transduced 6 h after replating with lentiviral vectors encoding GFP or the GFP-tagged viral proteins. In Fig. 2b, dimethylsulphoxide (DMSO) or 5 μM MLN4924 (Active Biochem) was added 6 h before transduction and culture medium was replaced daily with fresh medium containing (or not) MLN4924 for 3 days. In Fig. 2c, d and Extended Data Fig. 2f, g, cells were constantly grown in the absence or presence of 2 μg ml^{-1} doxycycline. Cell lysates were prepared 6 days later (3 days in Fig. 2b) for luciferase assay and western blot analysis. Luciferase activities were measured using the Luciferase Assay System (Promega) or Dual-Luciferase Reporter Assay System (Promega) according to the manufacturer's instructions. The activities were normalized to protein concentrations as measured by the Bradford assay (Bio-Rad).

Purification of Flag–StrepII-tagged proteins. The two-step purification scheme was adapted from ref. 29. The HepG2$^{tet\text{-}on}$ cell lines conditionally expressing FS-tagged proteins from a doxycycline-inducible promoter were seeded on thirty 15-cm dishes and allowed to reach 90% confluence. Expression of the FS-tagged proteins was then induced by addition of doxycycline (2 μg ml^{-1}) for 48 h. Cells were rinsed once with 20 ml PBS (per plate) and scraped off after incubation on ice for 20 min in 1.5 ml lysis buffer (50 mM HEPES/KOH, pH 7.5, 150 mM NaCl, 5 mM KCl, 5 mM $MgCl_2$, 50 μM $ZnCl_2$, 0.1% IGEPAL and protease inhibitor cocktail from Sigma). The lysates were pooled, supplemented with glycerol (10% final), and clarified by centrifugation at 20,000*g* for 20 min at 4 °C in a Sorvall HB-6 rotor. Supernatants were collected, passed through a 0.45 μm Millipore PVDF filter, and mixed in a 50 ml Falcon tube with a 100 μl packed bead volume of Strep-Tactin Sepharose (IBA) washed with lysis buffer. After incubation for 2 h at 4 °C under constant rotation, the suspension was poured into a 10 ml disposable column (Bio-Rad). After sedimentation, the resin was washed twice with 10 ml lysis buffer containing 10% glycerol. The bound proteins were released by incubating the resin with 10 ml of lysis buffer supplemented with 10% glycerol and 2.5 mM desthiobiotin (IBA 2× Tactin Elution Buffer) for 10 min on ice. The eluted material was directly mixed with a 100 μl packed volume of washed anti-Flag Sepharose beads (Sigma) and incubated with rotation for 1 h at 4 °C in a sealed 10 ml disposable column (Bio-Rad). Subsequently, the column was drained by gravity and the resin washed five times with 1 ml lysis buffer adjusted to 10% glycerol. Bound proteins were recovered by adding five times sequentially 200 μl lysis buffer supplemented with 200 μg ml^{-1} Flag peptide (Sigma) and gently mixing for 5 min on ice. The eluted material from three such purifications was pooled and precipitated with acetone (80% final concentration). After centrifugation at 4 °C in an Eppendorf microcentrifuge, the protein pellet was air-dried, resuspended in 1× Laemmli sample buffer, and run into a 4% SDS–PAGE stacking gel. The protein band was excised and processed for mass spectrometry analysis using an LTQ-Orbitrap Velos mass spectrometer (Thermo Scientific). Listed in Fig. 1b are proteins identified

with 99% certainty and represented by at least two peptides ascertained at a 95% confidence level.

In Fig. 1c, extracts from 6×10^6 HepG2 cells seeded on a 10-cm culture dish were prepared 2 days after transfection with 2 μg of EBS-PL expression plasmids. The experiment in Extended Data Fig. 1d was performed in the same way except that the transfected cells were selected in medium containing 200 μg ml^{-1} hygromycin B (PAA Laboratories) and extracts were prepared from a 15-cm dish of confluent cells. Proteins were purified by incubation with 25 μl packed bead volume of Strep-Tactin Sepharose (IBA).

Cell cycle analysis. The cell cycle analysis in Extended Data Fig. 3a was performed starting with 1.5×10^6 HepG2 cells transduced with GFP or GFP–HBx and cultured as above. Cells were harvested, washed once with PBS, and recovered by centrifugation at 500*g* for 5 min. Cells were fixed in 1 ml ice-cold 70% ethanol added dropwise while vortexing and incubated for 30 min on ice. The fixed cells were pelleted by centrifugation at 800*g* for 15 min, washed twice with PBS and directly resuspended in 50 μl PBS supplemented with 100 μg ml^{-1} RNase A (Roche). Cellular DNA was stained by addition of 600 μl of propidium iodide (Sigma Aldrich; 50 μg ml^{-1} in PBS) and incubation for 10 min at room temperature (20–25 °C) and overnight at 4 °C. Samples were analysed using a BD Accuri C6 flow cytometer.

Western blotting. With the exception of Fig. 4b and Extended Data Fig. 6g (see below), western blot analysis was performed as described[38] except that cells were disrupted in 2% SDS in water and protein concentration was estimated using the BCA Protein Assay (Novagen). The membranes were probed with 1:5,000 mouse anti-Flag antibodies (Sigma A2220) to detect the FS-tagged HBx–DDB1 and SV5-V–DDB1 fusion proteins, 1:5,000 mouse monoclonal anti-GFP (Roche 11814460001) to detect GFP–HBx in Extended Data Fig. 2a, b, 1:5,000 mouse monoclonal anti-HA (clone 16B12, Covance) to detect HA-Nse4 in Fig. 2e, 1:2,000 rabbit polyclonal antibodies against Smc5 or Smc6 (ref. 39) (a gift from A. R. Lehmann), 1:1,000 rabbit polyclonal anti-Nse4 (Abgent AP9909A), 1:2,000 rabbit polyclonal anti-Cardif/MAVS (Enzo Life Sciences ALX-210-929), 1:500 mouse monoclonal anti-STAT1 (BD Transduction Laboratories G16920), 1:500 goat polyclonal anti-DDB1 (Everest Biotech), 1:500 rabbit polyclonal anti-HBc (a gift from M. A. Petit), 1:500 mouse monoclonal anti-ubiquitin (Santa Cruz SC-8017), 1:10,000 mouse monoclonal anti-α-tubulin (Sigma-Aldrich T5168), or 1:10,000 mouse monoclonal anti-GAPDH (Sigma-Aldrich G8795) antibodies. Horseradish-peroxidase-conjugated sheep anti-rabbit or anti-mouse, or bovine anti-goat IgG (Amersham Biosciences, 1:5,000), were used as secondary antibodies, and detection was performed with ECL (Pierce).

In Fig. 4b, flash-frozen liver tissue from uPA-SCID mice re-populated with human hepatocytes was homogenized in RIPA buffer containing a broad spectrum protease inhibitor cocktail (Fisher Scientific PI-78430) using a Qiagen Tissue Lyser for mechanical tissue disruption. The resulting homogenates were clarified by centrifugation for 10 min at 4 °C in an Eppendorf 5415D microcentrifuge equipped with a fixed-angle rotor (F45-24-11) at 15,996*g*. Protein concentration was determined using the Bradford Protein assay (Bio-Rad). The membranes were probed with 1:1,000 mouse monoclonal anti-human SMC6 (Abgent AT3956A), 1:1,000 mouse anti-HBsAg (International ImmunoDiagnostics 1113), and 1:1,000 monoclonal mouse anti-human CK-18 (Dako M701029-2). IRDye 680RD goat anti-rabbit or IRDye 800CW goat anti-mouse IgG (Licor, 1:5,000) were used as secondary antibodies. Blots were visualized using an Odyssey Infrared Imaging System (Licor). The species specificity of the anti-human SMC6 and CK-18 antibodies was confirmed by western blot detection of Smc6 and CK-18 in HepG2 cells and PHHs but not in murine hepatocyte AML12 cells (ATCC CRL-2254, data not shown).

In Extended Data Fig. 6g, PHHs were lysed in RIPA buffer supplemented with 1× protease inhibitor cocktail (ThermoScientific), scraped from the plate, and sonicated for 10 s to break up cellular debris. Protein concentration was estimated using a BCA Protein Assay (Novagen). The membranes were probed with 1:1,000 mouse monoclonal anti-Smc5 (Bethyl Laboratories A300-236A), 1:1,000 mouse monoclonal anti-human SMC6 (Abgent AT3956A), 1:1,000 rabbit polyclonal anti-DDB1 (Cell Signaling 5428), and 1:1,000 mouse monoclonal anti-GAPDH (Novus Biologicals G8795). Secondary antibodies and detection were as in Fig. 4b.

RT–PCR analysis. In Extended Data Fig. 2c, total cellular RNA was extracted from HepG2 cells using TRIzol reagent (Invitrogen Life Technologies) following the manufacturer's instructions. RNA was treated with RNase-free DNase (Promega) in the presence of 1 U μl^{-1} RNAsin (Promega). After phenol/chloroform extraction and ethanol precipitation, 1 μg of RNA was reverse transcribed using MLV reverse transcriptase (Promega) and an oligo(dT)15 primer. Quantification by real-time PCR was performed as described[6]. The PCR values were normalized against those obtained for the TBP gene to correct for variation between samples.

In Extended Data Fig. 6e, f, i, total cellular RNA was isolated from PHHs cultured in 96-well plates using an RNeasy 96 Kit (Qiagen) following the manufacturer's instructions. Real-time RT–PCR was performed using a QuantStudio 7 Flex Real-Time PCR System (Invitrogen Life Technologies) following the manufacturer's instructions. The PCR values were normalized against those obtained for the β-actin gene to correct for variation between samples. All oligonucleotide primer sets were manufactured by Life Technologies.

Northern blot analysis. Northern blot analysis in Fig. 3c and Extended Data Fig. 6c was performed on total RNA isolated using TRIzol Reagent (Gibco-Invitrogen) and treated with RNase-Free DNase I (Ambion, Life Technologies). The RNA (10 μg per sample) was denatured by glyoxal treatment and separated on a 1% agarose gel using a NorthernMax-Gly kit (Ambion, Life Technologies). After capillary transfer to Hybond N$^+$ membranes (Amersham), the RNA was fixed on the membrane by ultraviolet cross-linking and hybridized with a ^{32}P-labelled full-length HBV genomic DNA or 28S ribosomal RNA oligonuclotide probes.

HBV virion production. The HBV producing HepG2 cell lines[4] were grown to confluence in DMEM/F12 as described above. When confluence was reached, cells were maintained in a 1:1 mixture of Dulbecco's modified Eagle's medium (DMEM) and Williams' E medium (Invitrogen Life Technologies) supplemented with 5% fetal calf serum, 7×10^{-5} M hydrocortisone hemisuccinate, 5 μg ml^{-1} insulin, and 1% DMSO. HBV-containing supernatants were collected every 2 days for 10 days. The supernatants were pooled, filtered through a 0.22 μm filtration unit (Merck Millipore), and concentrated by overnight precipitation with PEG 8000 (5% final) and centrifugation at 4 °C for 1 h at 6,000*g*. The viral pellet was resuspended in 1/50 of the original culture volume in PBS and sedimented at 4 °C through a 20 ml 10–20% sucrose gradient in PBS at 130,000*g* for 16 h in a SW32 Beckman rotor. The final pellet was resuspended in 1/100 of the original volume in William's E medium supplemented with 2% DMSO and 0.1% SVF and stored in aliquots at −80 °C. Infectious virus titre was estimated by real-time PCR quantification of the viral DNA recovered by immunoprecipitation with an excess of mouse monoclonal antibodies against the large envelope protein (preS1)[40]. Real-time PCR was performed using the SYBR Green PCR Master Mix (Roche Applied Science) and a LightCycler 480 system (Roche Applied Science) as described[34].

HBV virion production from HepAD38 cells was as follows. Cells were grown to confluence in DMEM/F12 supplemented with 10% fetal bovine serum (HyClone, Thermo Scientific), 1% non-essential amino acids, 50 μg ml^{-1} kanamycin, 200 μg ml^{-1} geneticin (all from Gibco Life Technologies), and 0.3 μg ml^{-1} tetracycline (Sigma-Aldrich). Once confluence was reached, the medium was exchanged for identical medium as above, but lacking tetracycline. After 10 days, the virus-containing medium was collected every 3–4 days for 21 days and stored at −80 °C. Subsequently, the aliquots were thawed, precipitated overnight at 4 °C using 6% PEG-8000 (Promega), and centrifuged at 4 °C for 15 min at 1,500*g*. Viral DNA was isolated using a DNeasy Blood & Tissue Kit (Qiagen). Viral titre was determined by real-time PCR.

PHH isolation and HBV infection. PHHs were isolated from resected normal human liver tissue using a two-step perfusion method and cultured as described[4,41]. PHHs were infected with PCR-normalized HBV virus stocks at a multiplicity of infection of 200–400 viral genome equivalents per cell[34]. The experiments in Fig. 3b, e and Extended Data Fig. 6e–i were performed using PHHs purchased from Life Technologies and maintained in William's E medium with added supplements as specified by the vendor. Cells were infected 24 h after plating on collagen-coated 96-well plates (BD Biosciences) with HepAD38-derived HBV virions at 500 viral genome equivalents per cell. In Extended Data Fig. 6g, cells were cultured on collagen-coated six-well plates (BD Biosciences).

Human liver chimaeric uPA-SCID mice. All animal work was performed by Phoenix Bio, in accordance with the Guide for the Care and Use of Laboratory Animals and approved by the Animal Ethics Committee of Phoenix Bio. Nine male uPA-SCID mice were transplanted at 16–23 days old with 1×10^6 PHHs from a single healthy donor as described[42]. After 10–13 weeks, six of these mice were infected by intraperitoneal injection with 5×10^5 genome equivalents of cell-culture-derived HBV genotype C. These animals were killed and serum and liver specimens were collected for measurement of HBV infection 14 weeks later. Serum HBV DNA reached a titre of $>1.5 \times 10^7$ copies per millilitre and serum HBsAg levels were $\geq 3.2 \times 10^2$ IU ml^{-1} in all infected animals. As a control, three of the nine mice were left uninfected. These animals were killed at 15 weeks after transplantation and then processed identically to the HBV-infected animals.

ELISA. The amounts of HBe and HBs antigens present in control and HBV-infected PHH culture media were determined at the indicated times by ELISA using Monolisa HBe Ag-Ab PLUS (Bio-Rad) and Monolisa anti-HBs PLUS (Bio-Rad) kits and a Chemiluminescence Immunoassay (Autobio Diagnostics) kit. In Fig. 3e and Extended Data Fig. 6h, ELISA was performed using an HBeAg EIA

(International Immunodiagnostics) kit and a SpectraMax M5 reader (Molecular Devices). Purified HBeAg was used as standard.

Immunofluorescence and confocal analysis. The proportion of PHHs infected with HBV in Fig. 3d and Extended Data Fig. 5 was estimated by confocal immunofluorescence microscopy for HBsAg expression[34]. PHHs were cultured and infected on collagen-I-coated glass slides. At 9–12 days after infection, cells were fixed with 3% paraformaldehyde in PBS and permeabilized with 0.1% saponin in PBS for 30 min at room temperature. Cells were stained with mouse monoclonal anti-HBs antibodies (a gift from M. A. Petit) diluted 1:200 in PBS containing 0.1% saponin and 3% bovine serum albumin (BSA). After washing in the same buffer, bound antibodies were detected using Alexa-Fluor-647-conjugated goat anti-mouse secondary antibodies (Invitrogen). After additional washes, the slides were mounted with fluorescence mounting medium (ProLong Gold, Life Technologies) and observed under a Leica SP5 X confocal microscope. Image analysis used ImageJ software.

Confocal analysis of Smc6 expression in HBV-infected and uninfected PHHs in Fig. 3b and Extended Data Fig. 7 was performed as follows. PHHs were seeded onto rat tail collagen-I-coated glass coverslips (Corning BioCoat 354089) at a density of 1.2×10^6 cells per well of a 6-well dish and allowed to adhere overnight. Cells were then mock-infected or infected at 500 viral genome equivalents per cell with wild-type HBV derived from HepAD38 cells. On day 13 after infection, the cells were washed twice with PBS and fixed in freshly prepared 4% paraformaldehyde (Electron Microscopy Services RT-15710) in PBS for 10 min at room temperature. After three washes in PBS, the cells were permeabilized in 1% TX-100 in PBS for 10 min at room temperature. Coverslips were incubated overnight at 4 °C in 3% normal goat serum (Jackson ImmunoResearch Laboratories 005-000-121) diluted in PBS to quench non-specific background. Coverslips were then inverted onto 100 µl droplets containing mouse anti-human SMC6 (Abgent AT3956a, 1:500) and polyclonal rabbit anti-HBcAg (Dako B0586, 1:1,600) diluted in 3% normal goat serum, and incubated at room temperature for 1 h. As a control, cells were reacted in parallel with purified mouse IgG2a isotype-matched control (Life Technologies MG2a00). After eight washes in PBS, coverslips were inverted onto 100 µl droplets of highly cross-adsorbed Alexa Fluor 488 goat-anti-mouse (Molecular Probes A11029) or Alexa Fluor 594 goat-anti-rabbit (Molecular Probes A11037) secondary antibodies diluted 1:200 in 3% normal goat serum, and incubated for 1 h at room temperature. Coverslips were washed eight times in PBS and rinsed in double-distilled water before mounting onto glass slides using Vectashield DAPI-containing hardening mounting medium (Vector Laboratories H-1500). Imaging was performed using an upright Zeiss LSM780 confocal system equipped with a ×63 objective lens (NA 1.4) and Zen software. All images within each sample set were captured using identical confocal settings. Images were adjusted for brightness and contrast using Adobe Photoshop CS6.

For immunofluorescence analysis of humanized mouse liver tissues, flash-frozen liver tissues was cryosectioned at a thickness of 5 µm onto microscope slides, fixed for 10 min in ice-cold 4% paraformaldehyde in PBS, and then washed three times in PBS. After one wash in Tween 20-containing AutoWash (BioCare Medical TWB945M), tissue sections were incubated with Rodent Block M solution (BioCare Medical RBM961L) for 30 min at room temperature, then stained overnight at 4 °C in a humidified chamber with mouse monoclonal anti-human Smc6 (Abgent AT3956a, 1:200) and rabbit polyclonal anti-HBsAg (Virostat 1811, 1:500) antibodies diluted in a 1:1 solution of Rodent Block M (BioCare Medical RBM961) and Renoir Red diluent (BioCare Medical PD904M). In parallel, re-population of liver tissue with human hepatocytes was evaluated by staining representative sections from each animal with goat anti-human albumin polyclonal antibodies (Bethyl A80-129A, 1:200), whose species specificity has been demonstrated[43], and for selected animals by co-staining with mouse monoclonal anti-human cytokeratin-18 antibody (Dako M7010, 1:25). Mouse IgG1 (Dako X0931) diluted in Dako Antibody Diluent S0809 served as a negative control (see Extended Data Fig. 9). After three 5 min washes in AutoWash buffer, tissue sections were reacted for 1 h at room temperature with Alexa Fluor 488 donkey anti-mouse and Alexa Fluor 594 donkey anti-rabbit secondary antibodies diluted 1:1,000 in PBS. Coverslips were applied using Vectashield DAPI-containing embedding medium (Vector Laboratories H-1500). Images were acquired using a ×40 objective lens (Fig. 4a) or a ×20 objective lens (Extended Data Fig. 8) and an inverted epifluorescence microscope (Leica DM LB) and arranged using Adobe Photoshop CS6. Note that imaging in Fig. 4a and Extended Data Fig. 8a was limited to areas completely re-populated with human hepatocytes, which were readily distinguished from poorly engrafted areas of mouse liver tissue on the basis of cellular morphology Extended Data Fig. 8b.

ChIP and quantitative PCR. The ChIP analysis in Fig. 2e was performed using chromatin extracted from about 7×10^6 HepG2 cells cultured in 100 mm diameter wells as above and expressing HA-Nse4 from a lentiviral vector. In Fig. 3f, freshly prepared PHHs were seeded into 75 cm^2 collagen-coated tissue culture flasks (10^7 cells per flask). Two days later, cells were infected with wild-type or HBx-mutant HBV particles. After culture for the indicated periods, cells were fixed with 1% formaldehyde (Sigma Aldrich 47608) for 10 min at 37 °C before quenching with 330 mM glycine. Cells were rinsed twice with ice cold PBS containing EDTA-free protease inhibitors (Roche) and 5 mM Na-butyrate, scraped off in 1.5 ml of the same buffer and collected by centrifugation. Cells were resuspended and lysed for 10 min at 4 °C in 1 ml Nuclear Extraction buffer (10 mM Tris-HCl (pH 8.0), 10 mM NaCl, 1% NP-40) supplemented with protease inhibitor cocktail (Roche). The nuclei were recovered by centrifugation at 500*g* for 5 min at 4 °C in an Eppendorf fixed-angle rotor (FA-45-18-11) and washed once in the same buffer. Nuclei were resuspended in 100 µl FA-lysis buffer (50 mM HEPES/KOH, pH 7.5, 140 mM NaCl, 1 mM EDTA, 1% Triton X-100) containing 1% SDS and incubated for 10 min at room temperature. After addition of another 100 µl FA-lysis buffer, the mixture was transferred to 1.5 ml bioruptor microtubes (Diagenode), and sonicated using a Diagenode Bioruptor Pico water bath sonicator (ten cycles of 15 s on and 30 s off at high setting). The sonicated lysates were clarified by centrifugation at 16,000*g* for 10 min and mixed in 800 µl FA-lysis buffer supplemented with protease inhibitors with 40 µl packed bead volume of protein A-Sepharose CL-4B (GE Healthcare) coupled to 4 µl anti-HA antibodies (clone 16B12, Covance) or 6 µl anti-Nse4 antibodies (Abgent AP9909A) and pre-incubated in FA-lysis buffer with sonicated salmon sperm DNA and BSA. After an overnight incubation at 4 °C under constant rotation, the beads were sedimented by brief centrifugation and the supernatant either discarded or in Extended Data Fig. 3c directly mixed and incubated overnight at 4 °C with anti-Nse4 affinity beads as above. The beads were washed twice with 1 ml FA-lysis buffer, twice with FA-lysis buffer adjusted to 500 mM NaCl and 0.5% sodium deoxycholate, and twice with 10 mM Tris-HCl buffer (pH 8.0) containing 1 mM EDTA, 250 mM LiCl, 1% NP-40, and 1% sodium deoxycholate. Bound protein–DNA complexes were released from the HA- and Nse4-affinity resins by incubation for 10 min at 65 °C in 200 µl buffer containing 100 mM Tris-HCl (pH 8.0), 1% SDS, 10 mM EDTA, and 10 mM EGTA. After addition of 200 µl Tris-EDTA (pH 8.0) and 60 µg proteinase K (Bioworld Technology), DNA crosslinks were reversed by overnight incubation at 65 °C. Samples were extracted twice with phenol–chloroform, once with chloroform, and then ethanol precipitated and resuspended in Tris-EDTA buffer. The input DNA treated identically and the recovered DNA were quantified in two separate real-time PCR runs using the KAPA SYBR FAST qPCR Kit Master Mix (2X) Universal (Kapa Biosystems) and the Bio-Rad CFX96 Real-time PCR System. The values were calculated as the ratios between the ChIP signals and the respective input DNA signals. In Fig. 3e, primers specific for the covalently closed circular HBV DNA (cccDNA)[14] were used. Sequences of the oligonucleotide primers are given in Supplementary Table 2.

Statistical analysis. No statistical methods were used to predetermine sample size. Statistical significance was tested using a one-tailed, paired *t*-test (for two sample comparisons) or one-way ANOVA with Dunnett's multiple comparison correction of log-transfomed data (for multiple comparisons). A value of $P < 0.05$ was considered significant. The experiments were not randomized, and the investigators were not blinded to allocation during experiments and outcome assessment.

Ethics statement. PHHs were isolated from liver specimens resected from patients undergoing partial hepatectomy (provided by M. Rivoire). Approval from the local and national ethics committees (French Ministry of Research and Education numbers AC-2013-1871 and DC-2013-1870) and informed consent from patients were obtained.

28. Lin-Marq, N., Bontron, S., Leupin, O. & Strubin, M. Hepatitis B virus X protein interferes with cell viability through interaction with the p127-kDa UV-damaged DNA-binding protein. *Virology* **287,** 266–274 (2001).
29. Gloeckner, C. J., Boldt, K., Schumacher, A., Roepman, R. & Ueffing, M. A novel tandem affinity purification strategy for the efficient isolation and characterisation of native protein complexes. *Proteomics* **7,** 4228–4234 (2007).
30. Bontron, S., Lin-Marq, N. & Strubin, M. Hepatitis B virus X protein associated with UV-DDB1 induces cell death in the nucleus and is functionally antagonized by UV-DDB2. *J. Biol. Chem.* **277,** 38847–38854 (2002).
31. Meerbrey, K. L. *et al.* The pINDUCER lentiviral toolkit for inducible RNA interference in vitro and in vivo. *Proc. Natl Acad. Sci. USA* **108,** 3665–3670 (2011).
32. De Iaco, A. & Luban, J. Inhibition of HIV-1 infection by TNPO3 depletion is determined by capsid and detectable after viral cDNA enters the nucleus. *Retrovirology* **8,** 98 (2011).
33. Goldring, C. E. *et al.* Development of a transactivator in hepatoma cells that allows expression of phase I, phase II, and chemical defense genes. *Am. J. Physiol. Cell Physiol.* **290,** C104–C115 (2006).
34. Hantz, O. *et al.* Persistence of the hepatitis B virus covalently closed circular DNA in HepaRG human hepatocyte-like cells. *J. Gen. Virol.* **90,** 127–135 (2009).

35. Ladner, S. K. *et al.* Inducible expression of human hepatitis B virus (HBV) in stably transfected hepatoblastoma cells: a novel system for screening potential inhibitors of HBV replication. *Antimicrob. Agents Chemother.* **41,** 1715–1720 (1997).
36. Kutner, R. H., Zhang, X. Y. & Reiser, J. Production, concentration and titration of pseudotyped HIV-1-based lentiviral vectors. *Nature Protocols* **4,** 495–505 (2009).
37. Rothe, M. *et al.* Epidermal growth factor improves lentivirus vector gene transfer into primary mouse hepatocytes. *Gene Ther.* **19,** 425–434 (2012).
38. Martin-Lluesma, S. *et al.* Hepatitis B virus X protein affects S phase progression leading to chromosome segregation defects by binding to damaged DNA binding protein 1. *Hepatology* **48,** 1467–1476 (2008).
39. Taylor, E. M. *et al.* Characterization of a novel human SMC heterodimer homologous to the *Schizosaccharomyces pombe* Rad18/Spr18 complex. *Mol. Biol. Cell* **12,** 1583–1594 (2001).
40. Chemin, I. *et al.* Correlation between HBV DNA detection by polymerase chain reaction and Pre-S1 antigenemia in symptomatic and asymptomatic hepatitis B virus infections. *J. Med. Virol.* **33,** 51–57 (1991).
41. Gripon, P., Diot, C. & Guguen-Guillouzo, C. Reproducible high level infection of cultured adult human hepatocytes by hepatitis B virus: effect of polyethylene glycol on adsorption and penetration. *Virology* **192,** 534–540 (1993).
42. Fujiwara, S. *et al.* A novel animal model for *in vivo* study of liver cancer metastasis. *World J. Gastroenterol.* **18,** 3875–3882 (2012).
43. Ishida, Y. *et al.* Novel robust *in vitro* hepatitis B virus infection model using fresh human hepatocytes isolated from humanized mice. *Am. J. Pathol.* **185,** 1275–1285 (2015).
44. Andrejeva, J. *et al.* The V proteins of paramyxoviruses bind the IFN-inducible RNA helicase, mda-5, and inhibit its activation of the IFN-beta promoter. *Proc. Natl Acad. Sci. USA* **101,** 17264–17269 (2004).

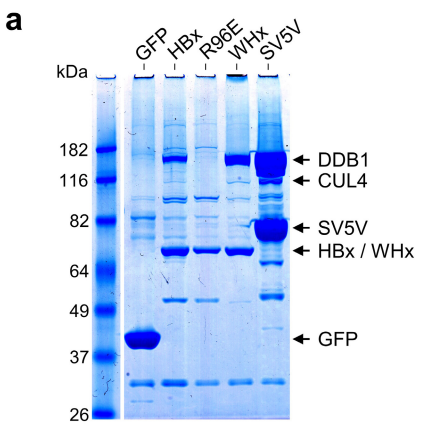

b

SV5-V	#pep	%cov
SV5-V	14	72
DDB1 E3 ligase		
DDB1	63	52
CUL4A	17	24
CUL4B	3	10
Other		
MDA5	14	18
HSC71	2	4

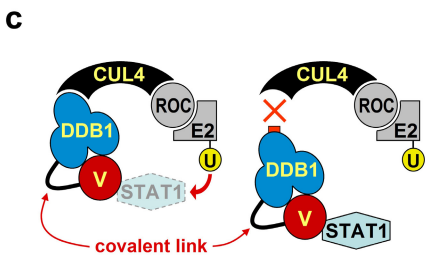

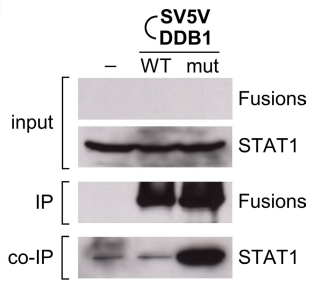

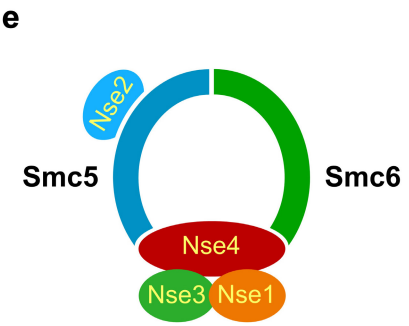

Extended Data Figure 1 | A strategy to identify E3 ubiquitin ligase substrates. a, Stable HepG2 cell lines were generated expressing GFP or the indicated GFP-tagged viral proteins carrying an N-terminal tandem Flag/StrepII (FS) tag from a doxycycline-inducible promoter (ref. 29 and see Methods). After doxycycline induction, whole-cell extracts were prepared and the FS-tagged and associated proteins were purified by TAP. Eluted proteins were separated by gel electrophoresis and stained with Coomassie blue. CUL4 was identified by mass spectrometry. No protein candidate was identified showing a profile predicted for an HBx substrate: that is, co-purifying specifically with HBx and WHx but not with SV5-V, or co-purifying only with the DDB1-binding-defective HBx(R96E) mutant because of its otherwise unstable interaction with HBx and WHx when recruited to the E3 ligase. In particular, the Smc5/6 complex was not detected in these purifications. **b**, Purification of SV5-V and associated proteins. FS-tagged SV5-V was purified from a stably expressing HepG2 cell line by TAP as above. Proteins were eluted under native conditions and processed for analysis by peptide fragmentation sequencing (nano-LC–ESI MS/MS). The number of unique peptides for each protein and the percentage of total protein sequence covered by these peptides are indicated. Listed are proteins identified with 100% certainty and represented by at least two peptides identified at a 95% confidence level. CUL4A and CUL4B are closely related paralogs. Note that no peptides were detected, even at low confidence level, for STAT1 that is well known to be recruited by SV5-V to the DDB1 E3 ligase for ubiquitin-mediated degradation. By contrast MDA5, a cytoplasmic sensor of viral RNA to which SV5-V also binds but, in contrast to STAT1, without causing its degradation[44], was present in the SV5-V purifications. This suggests that, in contrast to MDA5, STAT1 associates with SV5-V very transiently, presumably because of its rapid degradation or dissociation from the E3 ligase complex. We considered that the same may be true for the HBx target, thus precluding its identification by regular affinity purification. **c**, As a proof of principle for the use of a fusion strategy to identify the HBx target, we covalently linked SV5-V to wild-type DDB1 or to a CUL4-binding-defective DDB1 mutant that could not incorporate in the E3 ligase complex. See text for details. **d**, HepG2 cells were mock transfected (−) or transfected with plasmid DNA expressing the indicated FS-tagged SV5-V–DDB1 fusions. Whole-cell extracts were prepared and the fusion proteins purified by a single round of affinity purification. The amounts of fusion proteins recovered (IP) and the presence of STAT1 in the eluates (co-IP) were assessed by western blotting. The fusion proteins were revealed using anti-Flag antibodies and were expressed at too low levels for detection in the crude extracts (input). Note that high amounts of STAT1 are recovered only with the mutant SV5-V–DDB1 fusion. **e**, Architecture of the Smc5/6 complex. The core of the Smc5/6 complex is formed by a heterodimer of Smc5 and Smc6. The two proteins form a V-shaped structure and associate with four non-SMC proteins, designated Nse1–Nse4 (refs 15, 17). Note that depletion of any of the Smc5/6 complex subunit, other than Nse2, results in destabilization and degradation of the entire complex[21].

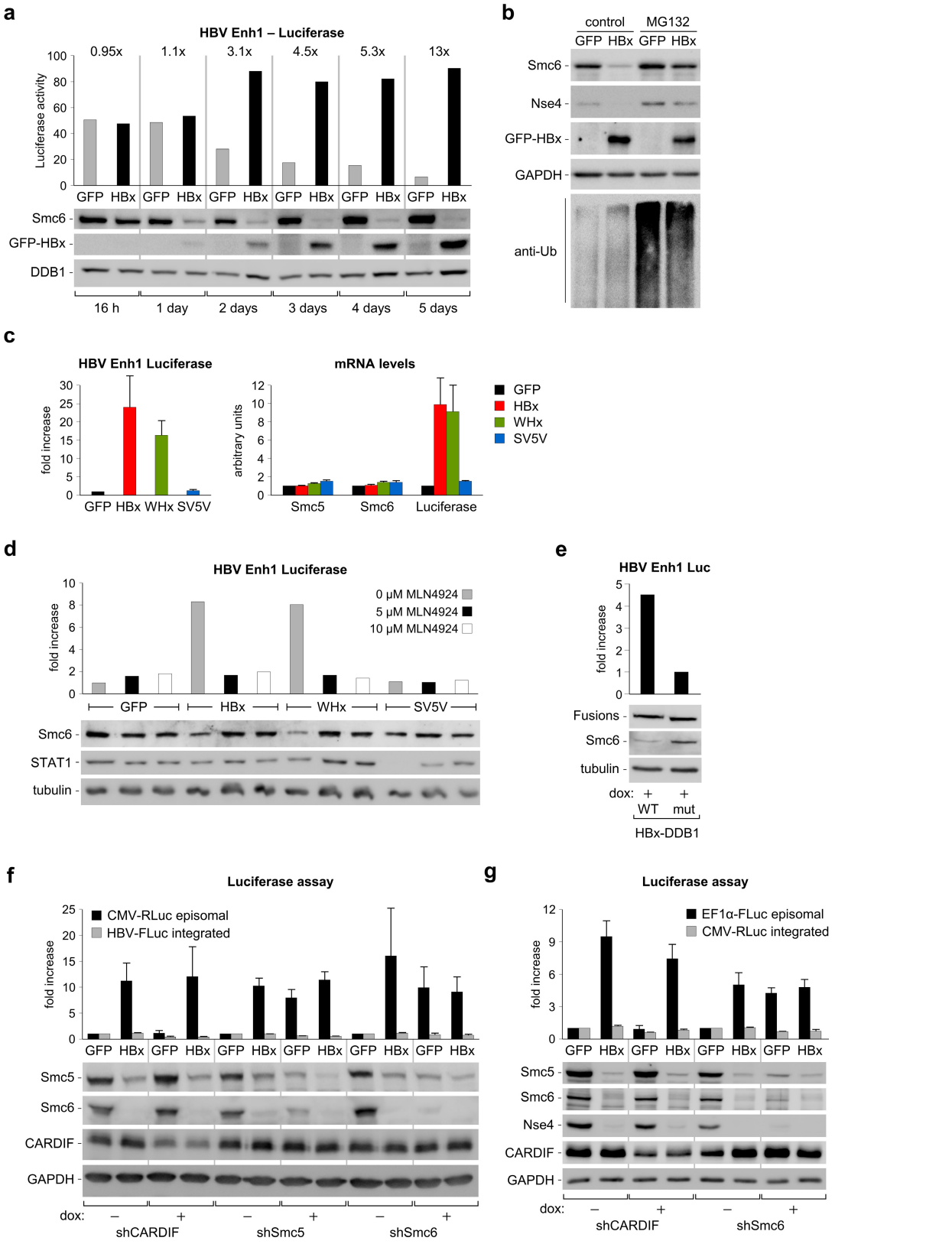

Extended Data Figure 2 | See next page for caption.

Extended Data Figure 2 | HBx induces rapid depletion of the Smc5/6 complex by an MG132 proteasome inhibitor-sensitive pathway to stimulate extrachromosomal reporter gene activity. a, Same experiment as in Fig. 2a except that luciferase activity and Smc6 protein levels were monitored at the indicated time points after transduction of GFP or GFP–HBx. Luciferase activities are expressed in arbitrary units, with the fold increase in HBx-expressing cells relative to GFP control cells indicated on top. GFP–HBx was detected using anti-GFP antibodies. One out of two independent experiments. **b**, HepG2 cells were transduced with lentiviral vectors encoding GFP or GFP–HBx. Then, 16 h later, DMSO (control) or 10 μM MG132 was added to the culture to inhibit proteasome activity. Cells were harvested 8 h later and the level of the indicated proteins and of global ubiquitination was analysed by western blotting. GFP–HBx was detected using anti-GFP antibodies. One out of two independent experiments. **c**, The effect of the indicated viral proteins on Smc5, Smc6, and luciferase mRNA levels was determined by real-time RT–PCR. The values are relative to those measured in GFP-transduced cells, which were set to 1. **d**, Similar experiment as in Fig. 2b except that two concentrations of MLN4924 were used. **e**, Similar experiment as in Fig. 2c. **f**, Similar experiment as in Fig. 2d but with HepG2 cells containing the HBV Enhancer-I-driven firefly luciferase reporter gene (HBV-FLuc) integrated into the chromosome and an episomal *Renilla* luciferase construct driven by the CMV promoter (CMV-RLuc). Note that the shRNAs against Smc5 and Smc6 used in this experiment differ from those in Fig. 2d (see Methods). **g**, Same with the *Renilla* luciferase CMV promoter construct chromosomally integrated and a firefly luciferase reporter gene driven by the EF1α promoter episomal. Data in **c**, **f** and **g** represent the mean ± s.e.m. of three independent experiments.

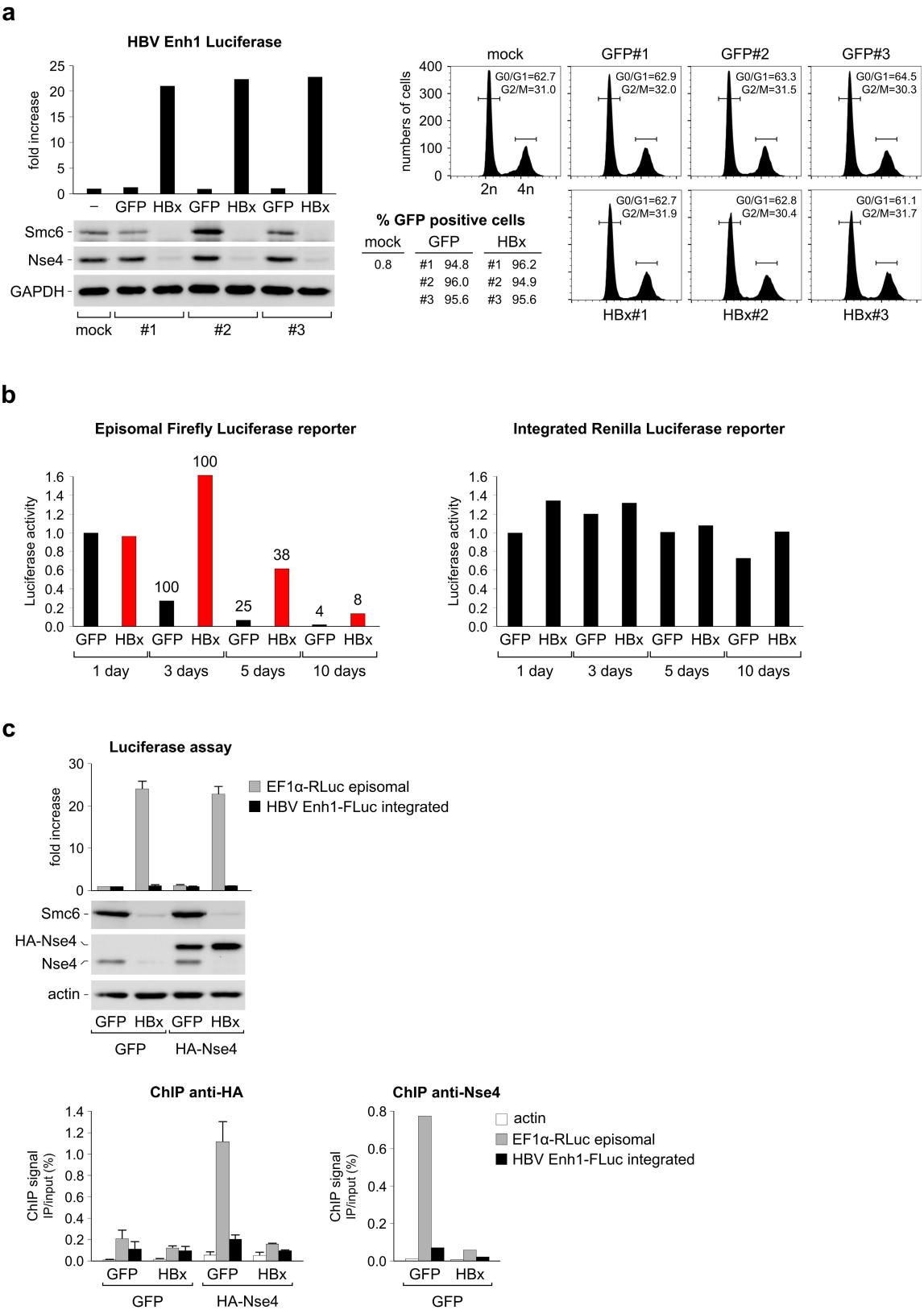

Extended Data Figure 3 | See next page for caption.

Extended Data Figure 3 | Smc5/6 degradation by HBx does not alter the cell cycle or promote chromosomal integration of the reporter but prevents the binding of Smc5/6 to the episomal DNA template. **a**, HepG2 cells were transfected with the HBV Enh1 luciferase reporter plasmid, split, and then either mock-transduced or transduced in triplicates with lentiviral vectors encoding GFP or GFP–HBx. Luciferase activity and protein expression (left panel) were monitored as in Fig. 2 at 5 days after transfection. In parallel, cells were analysed by FACS for GFP positivity (middle inset) and for DNA content (right panels) after propidium iodide staining. **b**, HBx does not promote stable integration of the reporter gene into chromosomes. HepG2 cells were transduced with a lentiviral vector to chromosomally integrate a *Renilla* luciferase reporter gene and subsequently transfected with a firefly reporter construct. Cells were then split equally and transduced with lentiviral vectors encoding GFP or GFP–HBx. Activity of the episomal firefly (left) and integrated *Renilla* (right) luciferase genes was monitored at the indicated time points after transduction of GFP or GFP–HBx. The values are expressed in arbitrary units relative to those measured at day 1 in the GFP control, which was set to 1.0. Indicated above the columns in the left panel is the remaining luciferase activity (expressed in per cent) relative to that measured 3 days after transfection. Note that in the absence of HBx (black bars in the left panel) the episomal firefly luciferase signal decreases rapidly with time, presumably because of loss of the reporter plasmid. In the presence of HBx (red bars in the left panel), the signal slightly increases to reach sixfold higher levels relative to the GFP control at 3 days after transfection, and then drops with kinetics close to that observed in the GFP control. In contrast, expression of the integrated *Renilla* reporter remains constant (right panel). This argues against HBx stimulating episomal reporter activity by promoting its integration into chromosomes. **c**, Left panels, the same ChIP experiment using anti-HA antibodies as in Fig. 2e but with HepG2 cells containing the HBV Enhancer-I-driven firefly luciferase reporter (HBV Enh1-FLuc) integrated into the chromosome and an episomal EF1α *Renilla* luciferase construct (EF1α-RLuc) as a control. Data represent the mean ± s.e.m. of three independent experiments. In one experiment, the unbound material from the indicated samples expressing no HA-tagged Nse4 was further purified using anti-Nse4 antibodies (lower right). Data are expressed as the percentage of input DNA recovered by ChIP. Note that in this experiment, the episomal reporter was delivered using an integrase-defective lentiviral vector[32].

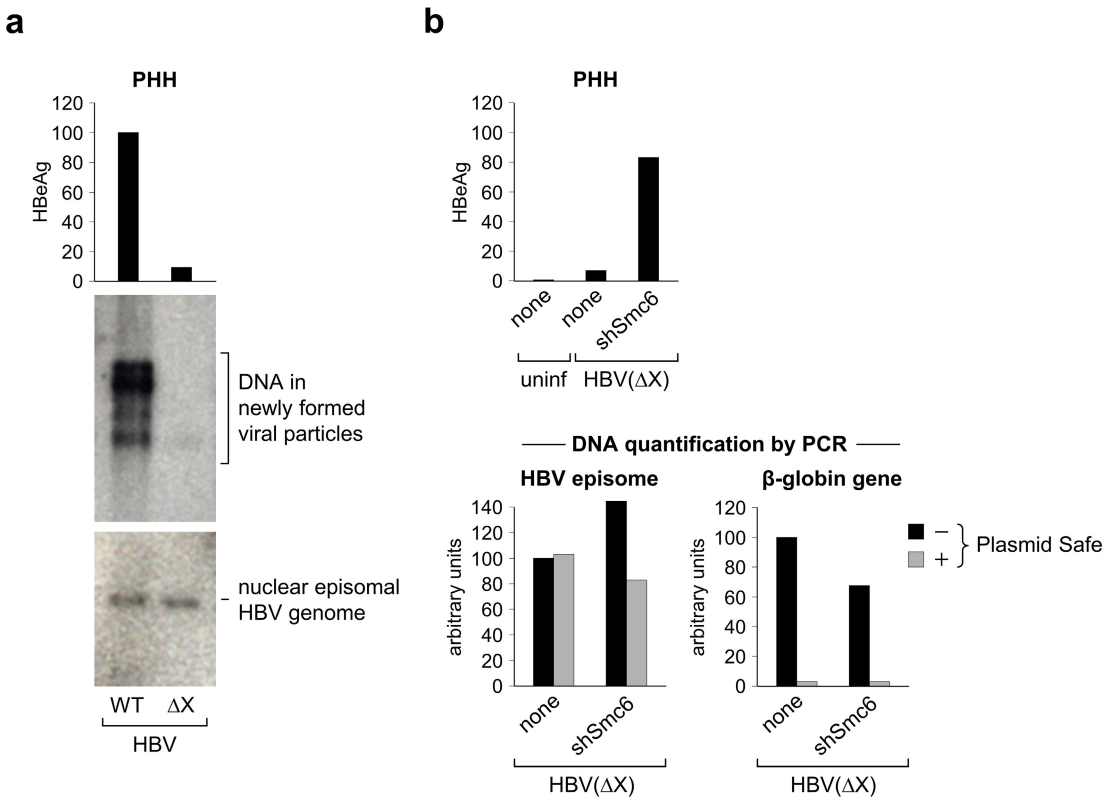

Extended Data Figure 4 | HBx or Smc5/6 knockdown does not affect HBV genome copy number. a, PHHs were infected with normalized stocks of wild-type (WT) or HBx-deficient (ΔX) HBV as in Fig. 3. HBeAg secretion (top) was assessed 10 days later by ELISA. In parallel, the amounts of cytoplasmic DNA replicative intermediates produced during reverse transcription of the viral pregenomic RNA (middle) and of the nuclear episomal HBV template extracted using a modified Hirt procedure (bottom) were analysed by Southern blot as reported[34]. **b**, PHHs were either mock transduced (none) or transduced with a lentiviral construct expressing an shRNA specific for Smc6 and the next day infected with HBx-deficient HBV particles (HBV(ΔX) as in Fig. 3c. HBeAg secretion was assessed 12 days later by ELISA (top). In parallel, the amount of nuclear HBV genome was quantified by real-time FRET–PCR[34] both directly or after treatment with Plasmid-safe DNase (Epicentre), an exonuclease that degrades single-stranded and double-stranded linear DNA but not the episomal HBV DNA (bottom left). Shown as a control for Plasmid-safe DNase treatment are the results for the chromosomal β-globin gene (bottom right).

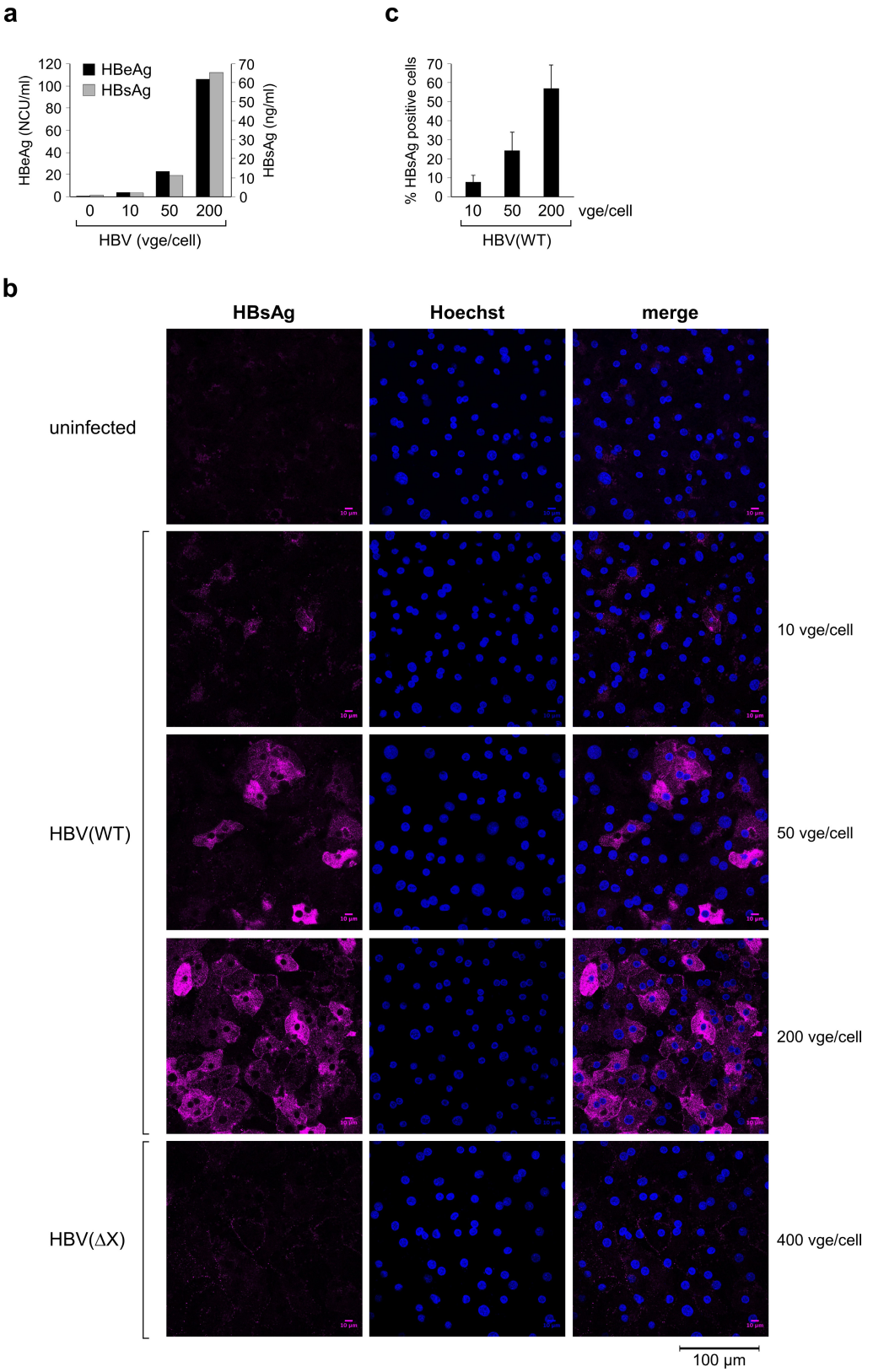

Extended Data Figure 5 | Efficiency of PHH infection by HBV. **a**, Purified PHHs were either left uninfected (0) or infected with wild-type HBV particles at the indicated viral-genome equivalents per cell (see Methods). HBeAg and surface antigen (HBsAg) secretion into the culture supernatants was assessed 10 days later by ELISA. Concentrations are expressed in, respectively, national clinical units (NCU) per millilitre (HBeAg) and nanograms per millilitre (HBsAg) and were determined according to the manufacturers' guidelines (Autobio Diagnostics). The noise signals measured with the supernatants from the uninfected cells were 0.50 NCU ml^{-1} and 0.88 ng ml^{-1}. **b**, PHHs infected with normalized stocks of wild-type (WT) or HBx-deficient (ΔX) HBV at the indicated viral genome equivalents per cell were examined for HBsAg expression at 9 days after infection by indirect immunofluorescence confocal microscopy. Cell nuclei were stained with Hoechst dye (blue). **c**, Quantification of confocal images. Data are mean ± s.d. of at least three fields. Note that infection in Fig. 3 was with 200 viral genome equivalents per cell or more.

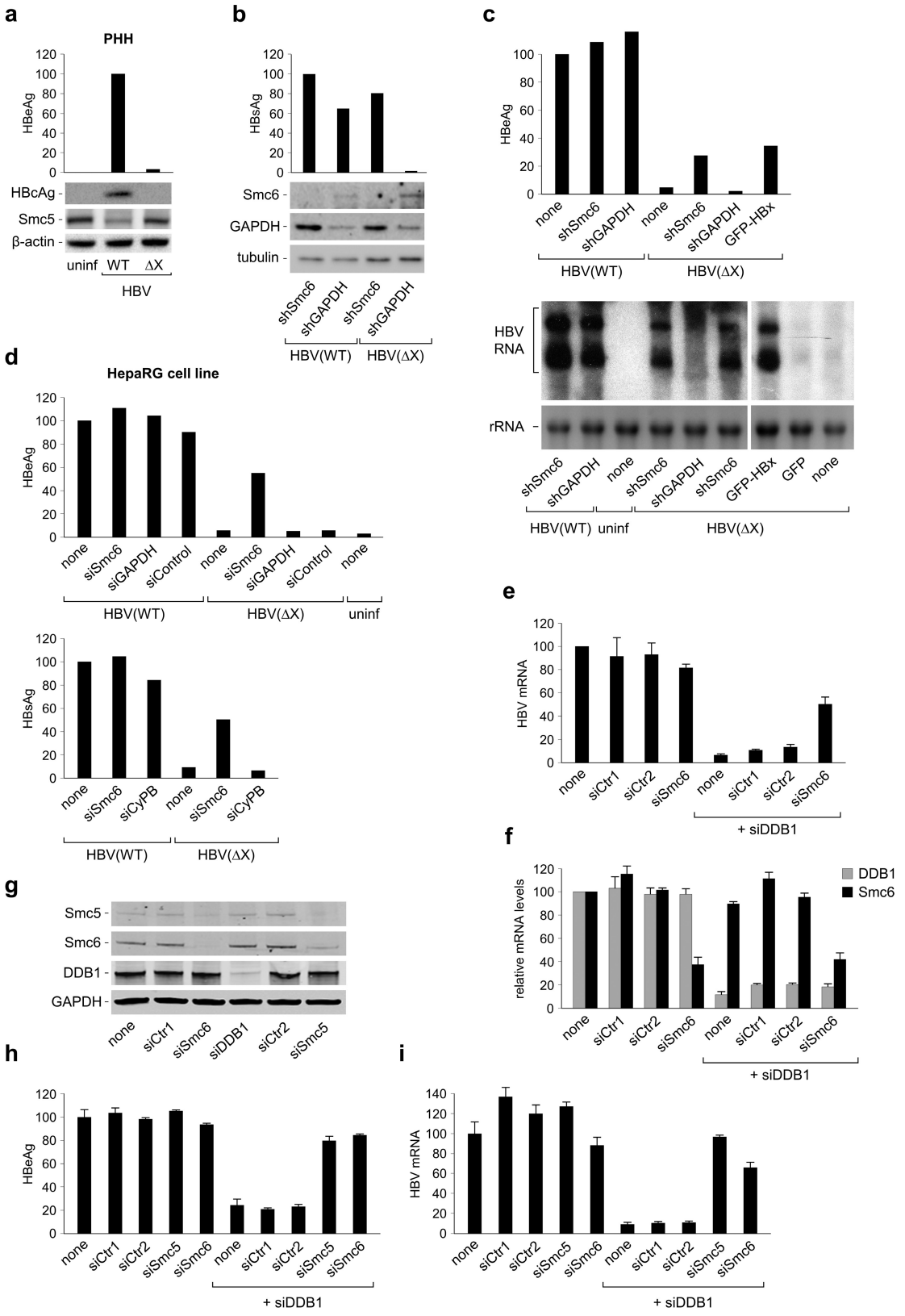

Extended Data Figure 6 | See next page for caption.

Extended Data Figure 6 | Silencing of Smc5/6 restores HBx-negative HBV transcription and rescues wild-type HBV on a DDB1 knockdown background. a, Biological replicate of Fig. 3a using PHHs from a different donor. **b**, Control for lentiviral shRNA-mediated depletion in PHHs. PHHs were transduced with lentiviral constructs expressing the indicated shRNAs and infected with HBV as in Fig. 3c. HBsAg secretion and the amounts of the indicated proteins were assessed 9 days later by ELISA and western blot analysis. HBsAg concentrations are relative to those measured in mock-transduced cells infected with wild-type HBV, which were taken as 100 (not shown). **c**, Independent northern blot analysis of HBV RNA production as in Fig. 3c using PHHs from a different donor. All lanes are from the same gel and exposure. Shown in the upper panel is the corresponding ELISA for HBeAg secretion. **d**, Smc5/6 silencing restores expression of HBx-negative HBV in HepaRG cells. Differentiated HepaRG cells were either left uninfected or infected with normalized stocks of wild-type (WT) or HBx-deficient (ΔX) HBV particles. Twenty-four hours later, cells were either mock transfected (none) or transfected with the indicated siRNA. HBeAg secretion was measured 10 days after infection by ELISA. The values are in arbitrary units relative to the wild-type HBV control, which was given a value of 100. Shown in the upper and lower panels are two independent experiments. CyPB, cyclophilin B. **e**, HBV mRNA expression. Total RNA was extracted from the samples analysed for HBeAg secretion in Fig. 3e. HBV mRNA levels were measured by real-time RT–PCR. The values normalized to β-actin are given in arbitrary units relative to those measured in mock-transfected cells, which were set to 100. Data represent the mean ± s.e.m. of $n = 4$ independent experiments performed with two different PHH donors. **f**, Control of siRNA efficacy. DDB1 (grey bars) and Smc6 (black bars) mRNA levels in Fig. 3e were measured by real-time RT–PCR and normalized to β-actin as in **e**. The values are given in arbitrary units relative to those measured in mock-transfected cells, which were set to 100. Data represent the mean ± s.e.m. of $n = 4$ independent experiments performed with two different PHH donors. **g**, Control western blot analysis of siRNA-mediated protein depletion. PHHs were transfected with the indicated siRNAs 3 days after plating. Protein levels were measured 10 days later. **h**, Data of one of the four experiments used in Fig. 3e that includes an siRNA targeting Smc5. Mean ± s.e.m. of triplicate measurements. **i**, Same experiment as in **h** but measuring HBV mRNA levels. Mean ± s.e.m. of triplicate measurements.

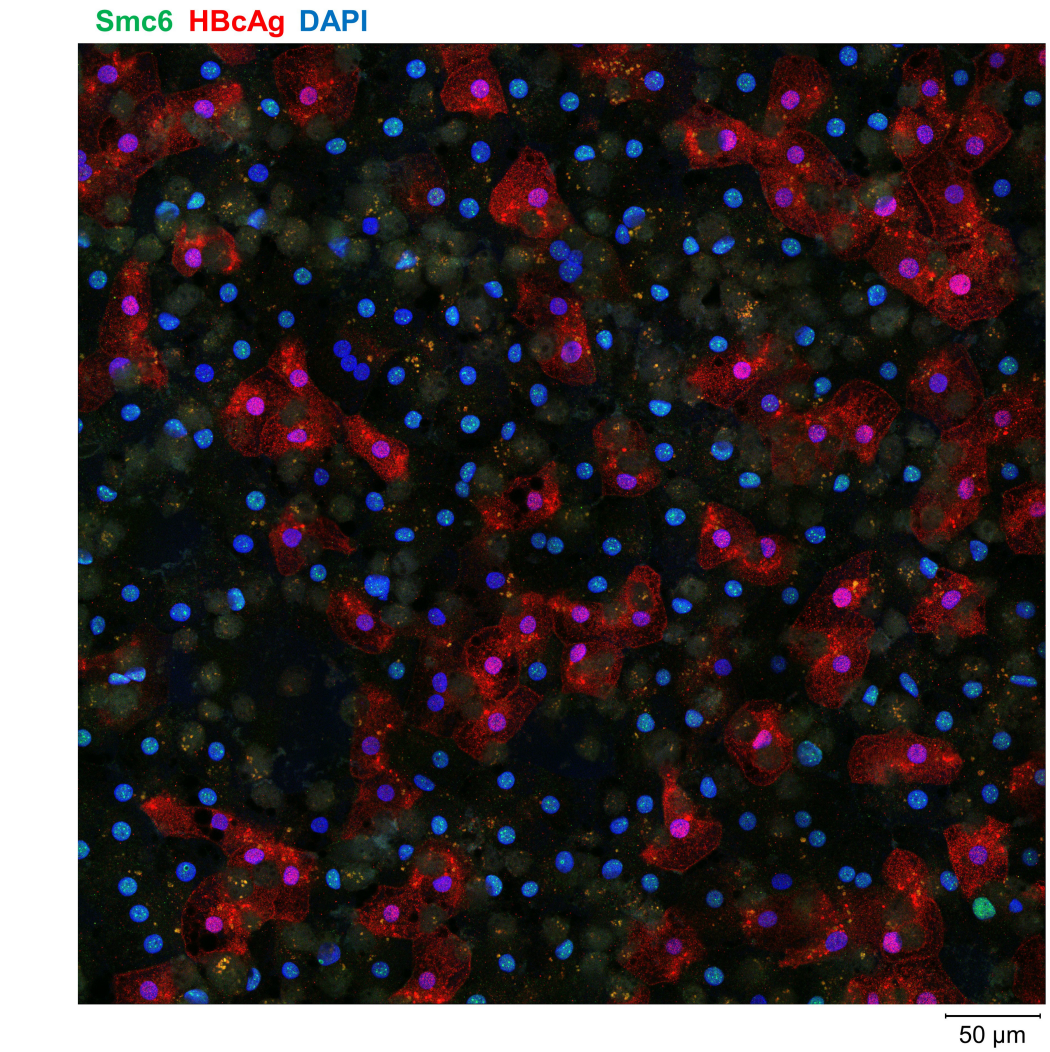

Extended Data Figure 7 | HBV infection induces Smc6 degradation in PHHs. a, Same as in Fig. 3b but 4 × 4 contiguous images were acquired and stitched together to produce a single image for examination of 200–300 PHHs. Shown are Smc6 (green), HBcAg (red), and DAPI (blue). **b**, Representative images of uninfected PHHs stained with mouse isotype-control-matched IgG2a primary antibodies or Alexa Fluor 488- and 594-conjugated secondary antibodies alone. Samples were imaged and processed as in Fig. 3b.

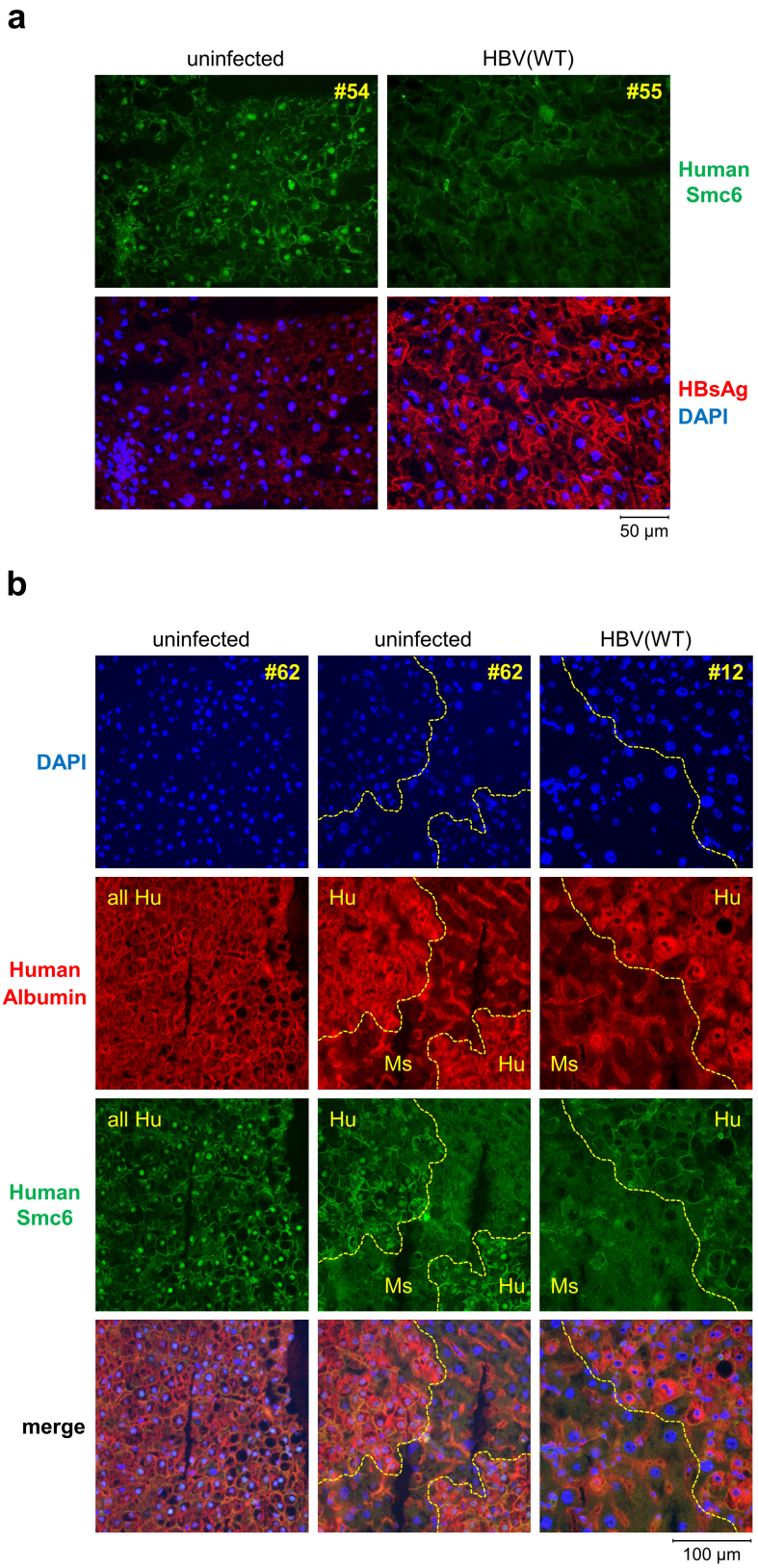

Extended Data Figure 8 | HBV infection induces Smc6 degradation in humanized mouse liver tissue. a, Same as in Fig. 4a but with different animal samples. **b**, Specificity of detection of human Smc6 in humanized mouse liver tissues. Fresh-frozen uninfected (animal 62) and infected (animal 12) humanized mouse liver tissues were stained with DAPI nuclear stain (blue) and with antibodies against human albumin (red) and human Smc6 (green). In the middle and right panels, a yellow dotted line delineates the interface between the human (Hu) and mouse (Ms) hepatocyte populations.

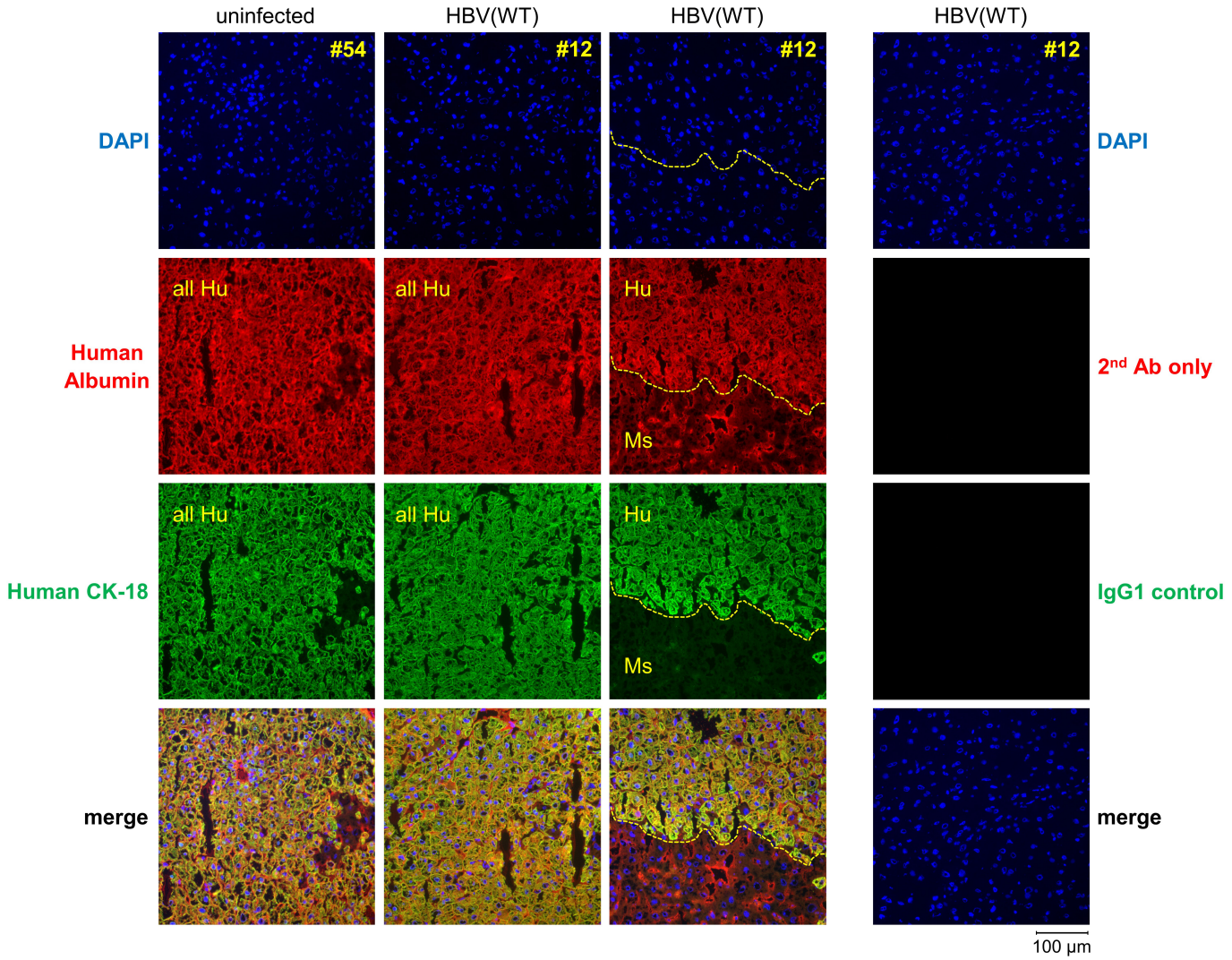

Extended Data Figure 9 | Human albumin and human cytokeratin-18 as markers for human hepatocytes in humanized mouse liver tissues. Fresh-frozen uninfected (animal 54) or infected (animal 12) humanized mouse liver tissues were stained with DAPI nuclear stain (blue) and with antibodies against human albumin (red) and human cytokeratin-18 (CK-18, green). A yellow dotted line delineates the interface between the human (Hu) and mouse (Ms) hepatocyte populations in the third column from left. Shown on the right are control staining of liver tissue from animal 12 with secondary antibody only or IgG1 isotype control.